NRC·CNRC

NRC Publications Archive
Archives des publications du CNRC

Characterization of low temperature mechanical propertis of crack sealants utilizing direct tension test

Al-Qadi, I. L.; Yang, S.-H.; Masson, J.-F.; McGhee, K. K.

For the publisher's version, please access the DOI link below./ Pour consulter la version de l'éditeur, utilisez le lien DOI ci-dessous.

https://doi.org/10.4224/20374662

NRC Publications Record / Notice d'Archives des publications de CNRC:
https://nrc-publications.canada.ca/eng/view/object/?id=1e206a79-2ff5-4334-a761-f9474d89a799
https://publications-cnrc.canada.ca/fra/voir/objet/?id=1e206a79-2ff5-4334-a761-f9474d89a799

Access and use of this website and the material on it are subject to the Terms and Conditions set forth at
https://nrc-publications.canada.ca/eng/copyright
READ THESE TERMS AND CONDITIONS CAREFULLY BEFORE USING THIS WEBSITE.

L'accès à ce site Web et l'utilisation de son contenu sont assujettis aux conditions présentées dans le site
https://publications-cnrc.canada.ca/fra/droits
LISEZ CES CONDITIONS ATTENTIVEMENT AVANT D'UTILISER CE SITE WEB.

Questions? Contact the NRC Publications Archive team at PublicationsArchive-ArchivesPublications@nrc-cnrc.gc.ca. If you wish to email the authors directly, please see the first page of the publication for their contact information.

Vous avez des questions? Nous pouvons vous aider. Pour communiquer directement avec un auteur, consultez la première page de la revue dans laquelle son article a été publié afin de trouver ses coordonnées. Si vous n'arrivez pas à les repérer, communiquez avec nous à PublicationsArchive-ArchivesPublications@nrc-cnrc.gc.ca.

National Research Council Canada | Conseil national de recherches Canada

Canada

NRC·CNRC Institute for Research in Construction
CNRC·NRC Institut de recherche en construction

http://www.nrc-cnrc.gc.ca/irc

Characterization of low temperature mechanical propertis of crack sealants utilizing direct tension test

NRCC-53257

Al-Qadi, I.L.; Yang, S.-H.; Masson, J.-F.; McGhee, K.K.

March 2010

A version of this document is published in / Une version de ce document se trouve dans:
llinois Center for Transportation, pp. 46, November 01, 2008

The material in this document is covered by the provisions of the Copyright Act, by Canadian laws, policies, regulations and international agreements. Such provisions serve to identify the information source and, in specific instances, to prohibit reproduction of materials without written permission. For more information visit http://laws.justice.gc.ca/en/showtdm/cs/C-42

Les renseignements dans ce document sont protégés par la Loi sur le droit d'auteur, par les lois, les politiques et les règlements du Canada et des accords internationaux. Ces dispositions permettent d'identifier la source de l'information et, dans certains cas, d'interdire la copie de documents sans permission écrite. Pour obtenir de plus amples renseignements : http://lois.justice.gc.ca/fr/showtdm/cs/C-42

National Research Council Canada | Conseil national de recherches Canada | Canada



CIVIL ENGINEERING STUDIES
Illinois Center for Transportation Series No. 08-028
UILU-ENG-2008-2016
ISSN: 0197-9191

CHARACTERIZATION OF LOW TEMPERATURE MECHANICAL PROPERTIES OF CRACK SEALANTS UTILIZING DIRECT TENSION TEST

Prepared By

Imad L. Al-Qadi
Shih-Hsien Yang
University of Illinois at Urbana-Champaign

Jean-François Masson
National Research Council of Canada

Kevin K. McGhee
Virginia Transportation Research Council

Research Report ICT-08-028

Illinois Center for Transportation

November 2008

Technical Report Documentation Page

1. Report No.	2. Government Accession No.	3. Recipient's Catalog No.
ICT-08-028		

4. Title and Subtitle
CHARACTERIZATION OF LOW TEMPERATURE MECHANICAL PROPERTIES OF CRACK SEALANTS UTILIZING DIRECT TENSION TEST

5. Report Date
November 2008

6. Performing Organization Code

7. Author(s)
Imad L. Al-Qadi, Shih-Hsien Yang, Jean-François Masson, Kevin K. McGhee

8. Performing Organization Report N o.
ICT-08-028
UILU-ENG-2008-2016

9. Performing Organization Name and Address

University of Illinois at Urbana Champaign
Department of Civil and Environmental Engineering
205 N. Mathews Ave, MC-250
Urbana, Illinois 61081

10. Work Unit (TRAIS)

11. Contract or Grant No.
VTRC Project # 67775
TPF-5(045)

13. Type of Report and Period Covered
Technical Report

12. Sponsoring Agency Name and Address

Federal Highway Administration
400 North 8th Street, Room 750
Richmond, VA 23219-4825

Virginia DOT – Lead State
1401 E. Broad St
Richmond, VA 23219

14. Sponsoring Agency Code

15. Supplementary Notes

16. Abstract

Crack sealing has been widely used as a routine preventative maintenance practice. Given its proper installation, crack sealants can extend pavement service life by three to five years. However, current specifications for the selection of crack sealants correlate poorly with field performance. The purpose of this research was to develop performance guidelines for the selection of hot-poured bituminous crack sealants at low temperature. This was accomplished by measuring the mechanical properties of crack sealant at low temperature and then developing performance criteria for material selection. The modified direct tension test (DTT), crack sealant direct tension test (CSDTT), simulates the in-situ loading behavior of crack sealants in the laboratory. A modified dog-bone specimen geometry, which allows specimens to be stretched up to 95%, is recommended. This new specimen geometry also facilitates sample preparation. Tensile force is applied to the dog-bone specimen, with its effective gauge length of 20.3mm, and is pulled at a deformation rate of 1.2mm/min. Fifteen sealants were tested at various temperatures, and three performance parameters are suggested as indicators of sealant performance: extendibility, percent modulus reduction, and strain energy density. Extendibility, which is used to assess the degree of deformation undergone by a sealant at low temperature before it ruptures or internal damage is observed, is recommended as a measured parameter to be included in the performance-based guidelines for the selection of hot-poured crack sealants. Extendibility thresholds were defined as function of low service temperatures. The CSDT is conducted at +6^{o}C above the lowest in service temperature because of the relatively high test loading rate compared to in-situ crack sealant movement rate.

17. Key Words	18. Distribution Statement
	No restrictions. This document is available to the public through the National Technical Information Service, Springfield, Virginia 22161.

19. Security Classif. (of this report)	20. Security Classif. (of this page)	21. No. of Pages	22. Price
Unclassified	Unclassified	69	

ACKNOWLEDGEMENT

The research on the Development of Performance-Based Guidelines for the Selection of Bituminous–Based Hot-Poured Pavement Crack Sealants is sponsored by the Federal Highway Administration “pooled-fund study TPF5 (045)” and the US-Canadian Crack Sealant Consortium. The contribution of the participating states, industry, and provinces is acknowledged. This report is part of a series of reports that resulted from this study. Four reports were published by the Illinois Center for Transportation:

Al-Qadi, I.L., E.H. Fini, H.D. Figueroa, J.-F Masson, and K.K. McGhee, Adhesion Testing Procedure for Hot-Poured Crack Sealants, Final Report, No. ICT-08-026, Illinois Center for Transportation, Rantoul, IL, Dec 2008, 103 p.

Al-Qadi, I.L., E.H. Fini, J.-F Masson, A. Loulizi, K.K. McGhee, M.A. Elseifi, Development of Apparent Viscosity Test for Hot-Poured Crack Sealants, Final Report, No. ICT-08-027, Illinois Center for Transportation, Rantoul, IL, Dec 2008, 41 p.

Al-Qadi, I.L., S.-H. Yang, J.-F. Masson, and K.K. McGhee, Characterization of Low Temperature Mechanical Properties of Crack Sealants Utilizing Direct Tension Test, Final Report, No. ICT-08-028, Illinois Center for Transportation, Rantoul, IL, Dec 2008, 70 p.

Al-Qadi, I.L., S.-H. Yang, M.A. Elseifi, S. Dessouky, A. Loulizi, J.-F. Masson, and K.K. McGhee, Characterization of Low Temperature Creep Properties of Crack Sealants Using Bending Beam Rheometry, Final Report, No. ICT-08-029, Illinois Center for Transportation, Rantoul, IL, Dec 2008, 81 p.

Two internal reports on aging and sealant characterization were published by the National Research Council of Canada and a summary can be found in the following papers):

Collins, P., Veitch, M., Masson, J-F., Al-Qadi, I. L., Deformation and Tracking of Bituminous Sealants in Summer Temperatures: Pseudo-field Behaviour, *International Journal of Pavement Engineering*, Vol. 9, No. 1, 2008, pp. 1-8.

Masson, J-F., Woods, J. R., Collins, P., Al-Qadi, I. L., Accelerated Aging of Bituminous Sealants: Small-kettle Aging, *International Journal of Pavement Engineering*, Vol. 9, No. 5, 2008, pp. 365-371.

In addition, an executive summary report of the study was published by the Virginia Transportation Research Council (the leading state of the study):

Al-Qadi, I. L. J-F. Masson, S-H. Yang, E. Fini, and K. K. McGhee, Development of Performance-Based Guidelines for Selection of Bituminous-Based Hot-Poured Pavement Crack Sealant: An Executive Summary Report, Final Report, No. VTRC 09-CR7, Virginia Department of Transportation, Charlottesville, VA, 2008, 40 p.

DISCLAIMER

The project that is the subject of this report was completed under contract with the Virginia Transportation Research Council, which served as lead-state coordinator and project monitor for the partner states of Connecticut, Georgia, Maine, Michigan, Minnesota, New Hampshire, New York, Rhode Island, Texas, and Virginia. The contents of this report reflect the views of the authors, who are responsible for the facts and the accuracy of the data presented herein. The contents do not necessarily reflect the official views or policies of the Virginia Transportation Research Council, the partnering states, the Illinois Center for Transportation, the Illinois Department of Transportation, the Federal Highway Administration, or the remaining members of the Crack Sealant Consortium. This report does not constitute a standard, specification, or regulation. Any inclusion of manufacturer names, trade names, or trademarks is for identification purposes only and is not to be considered an endorsement.

EXECUTIVE SUMMARY

Crack sealing has been widely used as a routine preventative maintenance practice. Given its proper installation, crack sealants can extend pavement service life by three to five years. However, current specifications for the selection of crack sealants correlate poorly with field performance. The purpose of this research was to develop performance guidelines for the selection of hot-poured bituminous crack sealants at low temperature. This was accomplished by measuring the mechanical properties of crack sealant at low temperature and then developing performance criteria for material selection. The modified direct tension test (DTT), crack sealant direct tension test (CSDTT), simulates the in-situ loading behavior of crack sealants in the laboratory. A modified dog-bone specimen geometry, which allows specimens to be stretched up to 95%, is recommended. This new specimen geometry also facilitates sample preparation. Tensile force is applied to the dog-bone specimen, with its effective gauge length of 20.3mm, and is pulled at a deformation rate of 1.2mm/min. Fifteen sealants were tested at various temperatures, and three performance parameters are suggested as indicators of sealant performance: extendibility, percent modulus reduction, and strain energy density. Extendibility, which is used to assess the degree of deformation undergone by a sealant at low temperature before it ruptures or internal damage is observed, is recommended as a measured parameter to be included in the performance-based guidelines for the selection of hot-poured crack sealants. Extendibility thresholds were defined as function of low service temperatures. The CSDT is conducted at +6^{o}C above the lowest in service temperature because of the relatively high test loading rate compared to in-situ crack sealant movement rate.

TABLE OF CONTENTS

EXECUTIVE SUMMARY ..... **IV**

INTRODUCTION **1**

PURPOSE AND SCOPE **2**

METHODS **3**

CRACK SEALANTS BEHAVIOR AT LOW TEMPERATURES 3
BITUMINOUS-BASED CRACK SEALANT—TYPES AND IDENTIFICATIONS 5
DIRECT TENSION TEST (DTT) FOR SUPERPAVE™ ASPHALT BINDER 6
Sealant Aging *8*
MODIFICATIONS TO THE SUPERPAVE™ DIRECT TENSION TEST 9
Test Development *9*
Stress Relaxation Test *10*
Middle Tension Notch Fracture Test *11*
Tensile Stress-Strain Test *13*
Test Procedure *20*
PERFORMANCE PARAMETERS 21
Strain Energy Density *22*
Percentage Modulus Decay *22*

RESULTS AND DISCUSSION **26**

EXTENDIBILITY 26
STRAIN ENERGY DENSITY (SED) 28
MODULUS DECAY PERCENTAGE 29

DISCUSSION **30**

SENSITIVITY ANALYSIS OF SPECIMEN GEOMETRY AND LOADING RATE ON STRESS-STRAIN RESPONSE 31
Effect of Cross-Section on Stress-Strain Response *32*
Effect of Specimen Length on Stress-Strain Response *32*
Loading Rate Effect on Stress-Strain Response *34*
TEMPERATURE EFFECT ON PERCENT MODULUS REDUCTION 35

TEST VARIATIONS **37**

CONCLUSIONS **40**

RECOMMENDATION **40**

ACKNOWLEDGMENTS ..... ERROR! BOOKMARK NOT DEFINED.

REFERENCES **42**

APPENDIX A **A-1**

CSDTT TESTING PROCEDURE A-1

APPENDIX B **B-1**

DETERMINATION OF EFFECTIVE GAUGE LENGTH FOR TEST SPECIMEN B-1

APPENDIX C **B-1**

SPECIFICATION B-1

FINAL CONTRACT REPORT

CHARACTERIZATION OF LOW TEMPERATURE MECHANICAL PROPERTIES OF CRACK SEALANTS UTILIZING DIRECT TENSION TESTER

Imad L. Al-Qadi
Founder Professor of Engineering
Illinois Center for Transportation, Director
Department of Civil and Environmental Engineering
University of Illinois at Urbana-Champaign

INTRODUCTION

ASTM standard D5535 defines a sealant as a material that possesses both adhesive and cohesive properties to form a seal, which prevents liquid and solid from penetrating into the pavement system. Crack sealing has been widely accepted as a routine preventative maintenance practice. Given its proper installation, crack sealant can extend pavement service life by a period ranging from three to five years (Chong and Phang, 1987). Numerous studies also demonstrated the cost effectiveness of crack sealants (Joseph, 1990; Cuelho et al. 2002, 2003; Fang et al. 2003; Ward 2001; Chong and Phang, 1987; Chong, 1990).

Crack sealant is produced so that it keeps its shape as applied and hardens through chemical and/or physical processes to form a viscoelastic rubber-like material that withstands extension or compression (crack movement) and weathering. However, in many cases, crack sealants may fail in one of two mechanisms at low temperature: cohesive or adhesive failure. The former occurs in the sealant, while the latter occurs at the sealant-pavement crack interface. At low temperatures, the sealant becomes more brittle because temperature might approach material's glass transition temperature and is subjected to short-duration loading due to crack movements associated with stick-slip motions and truck trafficking as well as long periods of environmental loading. Therefore, in order to achieve a cost-effective crack sealing/filling operation, two factors must be closely controlled: quality of sealant installation and sealant mechanical and rheological properties (such as viscosity, bulk stiffness, and adhesive bond strength). Both factors must be addressed in order to achieve the expected performance from the sealing/filling operation. Regardless of sealant quality, improper installation will cause premature failure and may lead to a shorter service life.

Over the past two decades, a new generation of highly modified crack sealants has been introduced to the market (Zanzotto, 1996). These sealants exhibit quite complex behavior compared to those of traditional sealant materials (Belangie and Anderson, 1985). Standards and specifications for selecting crack sealants have been established by several organizations, including American Society for Testing and Materials (ASTM), American Association of State Highway and Transportation Officials (AASHTO), and U.S. and Canadian federal, state, provincial, and municipal agencies. The objective of the specifications is to select materials that have the properties necessary to perform adequately in the field. Chehovits and Manning (1984) reported eight specific properties that are important for crack sealants:

1. Ability to be easily and properly placed in a crack through application equipment;
2. Adequate adhesion to remain bonded to hot-mix asphalt (HMA) crack wall;
3. Adequate resistance to softening and flow at high, in-service pavement temperatures so that the sealant will not flow from the crack, which will, therefore, prevent tracking;

4. Adequate flexibility and extendibility when crack is extended at low, in-service temperatures;
5. Sufficient elasticity to restrict the entrance of incompressible materials into the crack,
6. Sufficient pot life at application temperatures;
7. Resistance to degradation from weather to ensure long in-service life of the sealant; and
8. Compatibility with HMA, and low cure time to permit opening to traffic as soon as possible after application.

Current specification adopted by state DOTs and sealant manufacturers, ASTM D6690, are based on the flow test, the no-immersed bond test, the water-immersed bond test, the fuel-immersed bond test, the resilience test, the oven-aged resilience test, the asphalt compatibility test, the artificial weathering test, the tensile adhesion test, the solubility test, and the flexibility test. Such tests can be used to measure the consistency of crack sealants but cannot relate to sealant's performance. It has been widely reported by researchers that current specifications for selection of hot-poured crack sealants are based on tests whose results showed no correlation with field performance (Masson, 2000; Belangie and Anderson, 1985; Masson and Lacasse, 1999; Smith and Romine, 1993, 1999).

The most effective way to evaluate the performance of crack sealants would be to perform field tests. However, the results from field tests are sometimes controversial because a sealant can perform well in one site and fail in another simply because of differences in environmental conditions. Therefore, there is a definite need to develop a performance-based specification system to assist in the selection of crack sealants. Such a specification system would be based on sealant's performance-related parameters.

In this report, a sealant's ability to relax stress and its extendibility are investigated using the Direct Tension Tester (DTT). A sealant's ability to relax stress is critical at low temperatures since it determines how fast a sealant material can dissipate an imposed loading. A sealant experiences such loading when a crack expands and generates a tensile force upon the sealant. Extendibility is also important because when a crack opens, the sealant is expected to deform with the crack without failure. A typical crack movement may stretch the sealant from 10 to 100% strain (Smith and Romine, 1993; Masson and Lacasse, 1999; Linde, 1988; and Cook et al., 1990). In this research project, the DTT was selected for many reasons. This equipment applies a uniaxial monotonic load, which closely simulates the loading conditions due to crack movement in the field. Under these loading conditions, this equipment can maintain a temperature as low as -40^{o}C using a controlled environmental chamber. In addition, since this system is part of the SuperPave^{TM} binder specification system, a number of pavement and State agencies already own this equipment.

PURPOSE AND SCOPE

The objective of this project is to develop laboratory tests that measure sealant stress relaxation ability and extendibility, which may guide in the selection of sealant materials. Ultimately, the developed guidelines may enable the prediction of a crack sealant's performance for a particular site, with the benefit of being able to select more-durable sealants.

One of the major milestones of this study was to make use of the well-established equipment originally developed during the five-year Strategic Highway Research Program (SHRP), which was used for measuring binder failure behaviors as part of the performance grade (PG) system. This report describes the modified test method as well as the data analysis approach to characterize hot-poured bituminous-based sealant at low temperatures using the

SuperPave™ DTT device. This report also describes a testing program conducted on sealants, widely used in various geographic zones in North America, and the testing result analysis.

METHODS

Crack Sealants Behavior at Low Temperatures

In general, sealants are composed of asphalt binder, bitumen as the main component, and rubbery material such as styrene-butadiene copolymer, chemically modified crumb tire rubber, mineral filler and processing oil. The styrene-butadiene (SB) copolymer consists of linked blocks of polystyrene (PS) and polybutadiene (PB). The fillers may include crumb rubber block, rubber powder, or fibers. The variety of crack sealant chemical composition can significantly influence its rheological properties. Variations in the rheological properties can be attributed to different factors, including the source of the origin crude, the refining and modification process, and the content of polymer, filler, and additives.

The installed sealant material should have the appropriate rheological properties to resist crack movements, particularly during the winter season. Typically, there are two types of crack movements in the pavement: vertical and horizontal. Vertical movement primarily results from traffic loading on working cracks, and the horizontal movement is primarily due to thermal expansion and contraction of the pavement. Such pavement movement induces an external force on the crack sealant. While the load is imposed on crack sealant, as a viscoelastic material, sealant will tend to relax the imposed loading. If the stress inside the sealant builds up during loading is faster than the stress being relaxed, the un-relaxed stress will accumulate inside the sealant. If this accumulated stress is greater than the adhesive strength between sealant and crack walls but smaller than its cohesive strength, the material will fail in debonding. In contrast, if this accumulated stress is greater than sealant's cohesive strength but smaller than its adhesive strength, sealant will tend to fail in the bulk of the material. Therefore, the rate of external loading applied to the sealant should be considered in any laboratory test that simulates field conditions.

It has been widely recognized that low temperature critically affects the performance of crack sealant materials. When the temperature drops, the sealant stiffens due to physical hardening and cracks widen because of pavement contraction. Two mechanisms of failure may be evident during the crack widening process: cohesive failure, which occurs inside the sealant material and adhesive failure, which occurs between the sealant and crack wall. When a crack opens, tensile stress is applied on the sealant. The stress is carried by the sealant's adhesive and cohesive strength. If the sealant's cohesive strength is greater than its adhesive strength and the applied stress is greater than the adhesive strength, debonding will occur. On the contrary, if the sealant's cohesive strength is less than its adhesive strength and the applied stress is greater than the cohesive strength, cohesive failure will be observed. To stimulate loading conditions for sealants in the field, a monotonic uniaxial tension test is proposed, using the Direct Tension Tester (DTT) device.

Many research studies have conducted measurements to evaluate horizontal crack movement (Smith and Romine, 1993; Masson and Lacasse, 1999; Linde, 1988; and Cook et al., 1990). However, few attempts have been made to measure vertical crack movement because of the difficulties this posed. Masson and Lacasse (1999) measured the opening that occurred over a period of one year in various routed cracks in the City of Montreal. The treated cracks were in HMA overlaying concrete pavements and were exposed to air temperatures ranging from -40°C to 40°C. As shown in Table 1, transverse cracks could extend up to 16% per year. In general, crack movement is governed by crack direction with respect to traffic loading (Table 1). In addition, transverse cracks are more predisposed to opening than the longitudinal ones.

Table 1 Percentage of Crack Extension in Montreal (after Masson and Lacasse, 1999)

Crack Length, mm	Crack Movement			
	Transverse Crack, mm	Extension, %	Longitudinal Crack, mm	Extension, %
12	1.82	15.2	1.62	13.5
19	3.09	16.3	2.06	10.8
40	3.62	9.1	2.79	7.0

As a part of the Strategic Highway Research Program (SHRP), Smith and Romine (1993) conducted a study to evaluate the performance of various materials used to seal transverse and longitudinal cracks. The experimental program utilized 15 various sealants (hot- and cold-applied), which were placed at five different sites: Abilene, Texas; Elma, Washington; Wichita, Kansas; Des Moines, Iowa; and Prescott, Ontario. In that study, horizontal crack movements were measured. The study suggested that crack movement was affected by crack configuration (longitudinal versus transverse) and pavement design. Average crack movement, percentage of crack extension, and the rate of crack movement at various locations are presented in Table 2.

Table 2 SHRP-H106 Test Sites Investigating Crack Movements (after Smith and Romine, 1993)

Test Site	Pavement Type	Crack Movement (Mean ± Std. Dev.), mm	Mean Rate of Crack Movement, mm/°C	Extension, %	Mean Rate of Crack Movement, mm/min
Abilene	Conventional HMA with fabric interlayer	0.91 ± 0.51	0.057	5.7±3.2	2.77×10^{-4}
Wichita, East	Full-Depth HMA	2.03±0.9	0.145	12.7±5.6	5.27×10^{-3}
Wichita, West		1.63±1.06	0.136	10.2±6.6	4.94×10^{-3}
Elma	Full-Depth HMA	1.04±0.42	0.13	6.5±2.6	N/A
Des Moines	Composite HMA/JRC	1.52±0.94	0.058	9.5±5.9	7.94×10^{-4}
Prescott	Composite HMA/JPC	1.17±0.35	0.03	7.3±2.2	N/A

Linde reported an extensive study on measuring crack movements in various airports and highway pavements in Sweden (Linde, 1988). A summary of data from five airports is presented in Table 3. The study results include the following: (1) short-term measurements (up to 24hrs) yield an average crack movement of approximately 4×10^{-2}mm/°C or 10^{-3}mm/min; (2) long-term measurements yield an average crack movement ranging from 0.4 to 1.25mm/°C or 5×10^{-5} to 8×10^{-4}mm/min; (3) the greatest crack movement from a reference point was 25mm over approximately 100 days; (4) the reference point does not return to its zero position (the reference point varied by as much as 5mm during four years); and (5) crack movements ranged from 0.12 to 0.17mm per meter of crack/joint spacing.

Table 3 Rate of Crack Movement and Extension Percentage at Five Swedish Airports (after Linde, 1988)

Type of Movement	Rate of Crack Movement			Max. Extension, %
	mm/°C	mm/min	%/min	
Daily	0.04	0.001	0.0079%	100
Yearly	0.4~1.25	$5x10^{-5}$~$8x10^{-4}$	0.0004~0.0063%	

A study conducted by University of Cincinnati at three test sites; pins and PK nails were installed to measure crack openings (Cook et al., 1990). As predicted, it was found that most cracks opened up as temperature decreased and closed as temperature increased. However, some crack movements did not follow the expected pattern and barely moved when temperature changed. The maximum reported crack extension was 2.5mm, which is equivalent to 100% extension. In general, crack extensions varied from 6% up to 100% and the rate of crack movement varied from 0.0004% to 0.04% per min.

In order to better simulate in-situ sealant service condition and to make use of the equipment developed by SHRP, some modifications were necessary to allow for the testing of hot-poured sealants. In addition, various sealant types that may be used in North America should be considered in the testing program.

Bituminous-Based Crack Sealant—Types and Identifications

Sealants with varying chemical compositions were selected for this study to validate the proposed performance-based selection guidelines. These sealants represent a wide array of rheological behavior and they are expected to be used in various locations in North America. Sealant products used at University of Illinois were designated by a two-character code, which identifies the sealant type (Table 4). Those sealants with one character code are those sealants, which were included in the field trials conducted in Canada. The field sealants were installed in the early 1990s, and were sampled in the unaged (V) condition and after 1 (w1), 3 (w3), 5 (w5), and 9 (w9) years of weathering. For example, sealant A was installed in Montreal, Canada in 1990. While sealants were installed, portions of the virgin sample were cut and designated as A_V. A virgin sealant that was aged in the lab according to the acceleration aging procedure developed under this project is designated as A_AV. Field samples of sealant A were taken at year 1, 3 and 5 years after installation and they were designated as A_w1, A_w3, and A_w5. On the other hand, although the field performance of some of the selected sealants was not known, they provided the research team with a wide array of rheological behaviors ranging from very soft to very stiff crack sealants.

Table 4 Sealants Description and Designation

ID	Notes	Penetration 25°C (dmm)	Flow 60°C (mm)	Resilience 25°C
QQ	Stiffest crack sealant	22	0	36
EE	Expected high temperature grade is -22°C	47	0	51
ZZ	Used in San Antonio, TX	42	N/A	N/A
YY	Used in San Antonio, TX	42	N/A	N/A
AB	Used in San Antonio, TX	40	N/A	23
VV	Modified with fiber	N/A	N/A	N/A
UU	SHRP H106 field data	62	1.5	N/A
AE	Widely used in NY, VA, and NH	N/A	N/A	N/A
DD	Expected low temperature grade is -34°C	80	1.5	50
MM	For aging study	120	1	70
WW	Field data available	N/A	N/A	N/A
NN	Field data available	75	0	70
AD	SHRP H106 field data available	N/A	1	80
PP	Field data available	130	1	44
BB	Softest crack sealant	148	0	80
SS	For preliminary test	122	0.1	63
CC	Field data available	N/A	0	65
GG	For preliminary test	66	0	75
HH	SHRP H106 field data	N/A	0	44
A	Field data available	86	0.5	57
B	Field data available	68	0.5	64
C	Field data available	78	0	59
E	Field data available	124	1	73
G	Field data available	50	0.5	51
J	Field data available	66	6	48

Direct Tension Test (DTT) for SuperPave™ Asphalt Binder

The Direct tension Test (DTT), which was originally introduced in 1992 as part of the original SuperPave™ binder specification system, is used to measure the tensile failure properties of asphalt binder at low temperatures. After several modifications, a new SuperPave™ DTT was introduced in 1995. This new system, which is very compact compared to the original system, utilizes a fluid-based temperature control system and was reported to produce accurate results (Dongre et al., 1997). The DTT test applies a uniaxial tensile loading to the specimen in a controlled environmental chamber, which closely simulates the loading conditions experienced by crack sealants in the field.

In the DTT test, dog-bone-shaped specimens are placed in a fluid medium kept at the desired temperature and pulled in tension until rupture occurs (Figure 1). The SuperPave™ specification system is only designed to determine the strain at failure to ensure that it is greater than 1%. However, with appropriate modifications to the software, the equipment is capable of determining the stress-strain curve in a uniaxial state of stress and other useful parameters.



Figure 1. The direct tensile tester and dog-bone specimen.

Figure 2 illustrates the SuperPave™ specimen geometry and the loading mechanism. For binder specifications, a constant rate of 1.0mm/min is used. The elongation of the tested specimen, the load applied to the specimen, and the bath temperature are measured and acquired by the equipment's data acquisition system. The dog-bone–shaped specimens are 100mm in overall length, including the end inserts. The asphalt portion of the specimen is 40mm long with an effective gauge length of 33.8mm. The specimen is 6mm wide and 6mm thick, which means that the specimen cross-sectional area is 36mm^2. The failure stress and strain are computed using Equations (1) and (2), respectively:

$$\sigma_f = \frac{P_f}{A_0} \quad (1)$$

$$\varepsilon_f = \frac{\Delta L_f}{L_0} \quad (2)$$

where,

σ_f = failure stress;
P_f = measured load at failure;
A_0 = original cross-sectional area (=36mm^2);
ε_f = failure strain;
ΔL_f = measured elongation at failure (ΔL); and
L_e = gauge length.

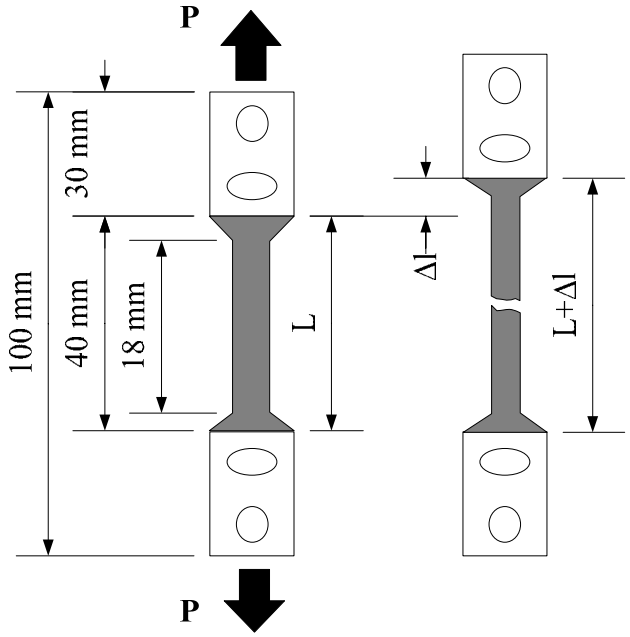


Figure 2. Sample geometry in the DTT setup.

Failure is defined as the point on the stress-strain curve where the load reaches its maximum (Figure 3). The test method was designated for asphalt binders at temperature where they exhibit brittle or brittle-ductile failure. The brittle or brittle ductile failure will result in a fracture of the test specimen as opposed to a ductile failure in which the specimen simply stretches without failure. Failure is defined in the SuperPave™ binder specification as when the tensile load (or stress) reaches a maximum. Failure may occur when the specimen fractures as in curve B or the specimen may continue to stretch after the maximum load as in curves C and D in Figure 3. Binder specification indicates that the minimum failure strain has to be greater than 1%, therefore, curve A will be rejected according to the specification (Anderson et al., 1994).

Sealant Aging

In the SuperPave ™ binder specification, the test is conducted on aged binder. Similarly, when a crack sealant is tested, it also requires aging the sealant prior to testing. In the SuperPave™ binder test, the Rolling Thin Film Oven (RTFO) and Pressure Vessel Aging (PAV) are used to simulate binder's short-term and long-term aging in the field. For crack sealants, a different aging procedure is adopted than that used for asphalt binder. The vacuum aging procedure is used to simulate crack sealant aging in the field. Details of this approach is presented in "Guidelines for Accelerated Aging of Bituminous Sealants Using a Vacuum Oven" (Masson et al., 2004). The vacuum aging procedure is used as one test for short- and long-term aging because most of sealant aging takes place during the installation process. In this method, homogenized sealant is sliced and placed in PAV pans. The pans are in a preheated oven at 180°C for approximately 5min to allow sealant to melt. The sealant film must be approximately 2-mm-thick. Once the melted sealant cool down to room temperature, the pans are placed in vacuum oven preheated to 115°C and vacuum is applied. When the vacuum reaches 760mm of mercury, the sealant is kept for 16hr.

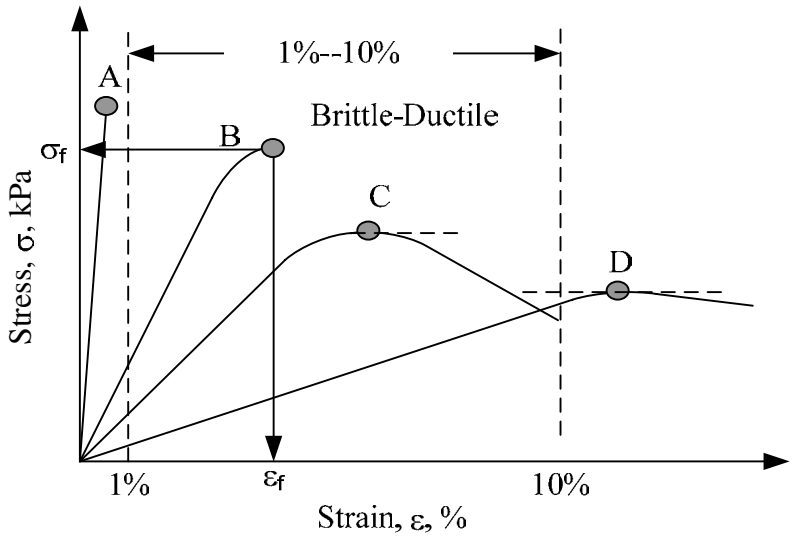


Figure 3 Various stress-strain behaviors of binder observed in the direct tension test

Modifications to the SuperPave™ Direct Tension Test

Test Development

Sealant is usually exposed to high temperature fluctuation; especially in the winter season. To evaluate their performance, a test procedure is needed that provides a connection between laboratory and field behaviors. Such test procedure is expected to be based on complex relations between various factors that govern sealant behavior. However, the developed test procedure should be relatively simple to be easily implemented by a state specification system. The factors controlling sealant performance include stress, strain, temperature, rate of deformation, humidity, air, light, type and condition of substrate, and presence of water or chemicals. Among these, the stress, strain, deformation rate, and temperature are of primary importance. They have to be known to describe the material behavior at any given age, humidity, substrate condition, etc. As a result, the sealant mechanical properties should be measured in any test developed, while all other factors should be kept constant at values considered to be realistic.

Cyclic test, tension stress-strain test, stress relaxation test, and fracture test are four common types of test used to obtain the material properties of polymers. The cyclic test is an excellent test which provides the best representation of crack sealant condition in the field. However, it is a very complex test and can be performed only if the material properties are well defined from the results of tests using simpler loading patterns and if the rates are related to the field. Therefore, it was not considered in this study.

Tension stress-strain test, stress relaxation test, and fracture test were evaluated. In the stress relaxation test, a specimen is rapidly stretched to the required length and the stress is recorded as a function of time. The stress relaxation test may cause serious damage to the material; but it usually does not result in real fracture. Tension stress-strain test and fracture test are used to evaluate sealant deformation and fracture properties. In the tensile stress-strain experiment, a specimen is elongated at a constant rate until it breaks. The stress is recorded as a function of extension. The middle notch tension fracture test is one of the most common type fracture tests to determine the characteristic energy and stress intensity

parameters widely used in fracture mechanics. The following sections describe each of the aforementioned approaches.

Stress Relaxation Test

The stress relaxation test consists of applying a rapid stretch stress on a material to a fixed length then records the stress as a function of time. Figure 4 illustrate a typical stress relaxation test. The stress relaxation has been related to the field performance of bituminous sealants (Zanzotto 1996). The original DTT software did not allow for stress relaxation experiments, so an upgrade of the software (TestBuilder) was purchased from the manufacturer. With the new software, sealant specimens were elongated to a predetermined elongation at a rate of 1mm/min (3% per min); then the elongation was kept constant for 15min, and the load needed to keep that elongation was recorded. Sealant BB, NN and QQ were selected for a feasibility evaluation because they represent soft, intermediate, and stiff sealants.

Replicates of Sealant QQ were tested at -10°C. The sealant was found to fail at -10°C at approximately 0.8% strain. Therefore, an elongation of 0.15mm (0.44% strain) was used (Figure 5). The maximum load was approximately 50N, which had relaxed to almost 5N after 15min. Replicates of Sealants BB and NN were also tested at -40°C. An elongation of 6mm (17.8% strain) was used for both sealants (Figure 5). The maximum load for Sealant BB was 13.2N, which decreased to 2.8N after 15min of relaxation. For Sealant NN, the maximum measured load was 38.8N, which decreased to 8.5N after relaxation. With a maximum travel distance of 13.5mm when using specimens in accordance with SuperPave™, an elongation as high as 12mm (35.5% strain) could be used in a stress relaxation test.

Although the stress relaxation could be performed on crack sealant materials, some limitations were observed. First, the rate to stretch the specimen was not rapid enough. For some sealant, the 1mm/min rate was too fast that adhesive failure results at the end tab; however, for some other sealants, this rate was too slow; hence, the sealant had significant relaxation going on prior to reach the predetermined length and the results might not reveal the true relaxation characteristics of these sealants. Second, the predetermined length varies for various sealants. Therefore, there was no unique length that could be used for the sealants considered in this study. This might cause inconsistency in the specification test. As a consequence of these findings, the stress relaxation test was not further considered as a potential test in this study.

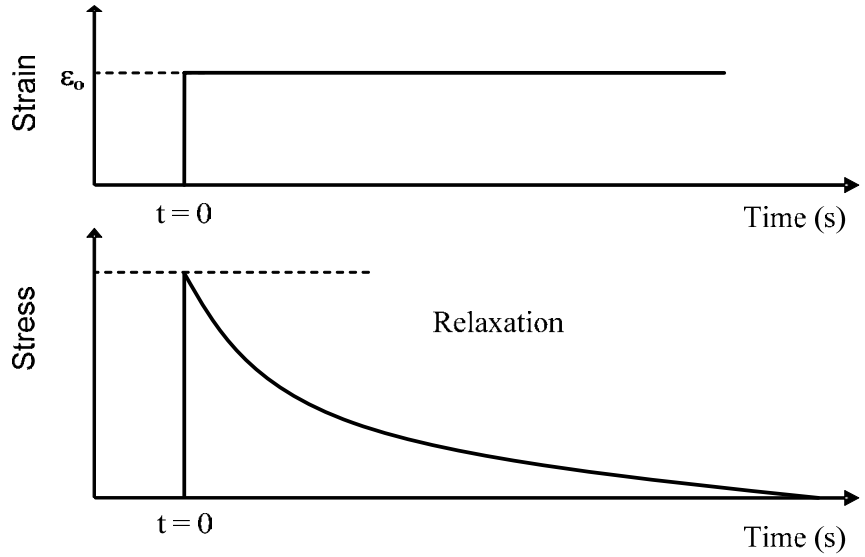


Figure 4. Schematic representation of stress relaxation for a viscoelastic material

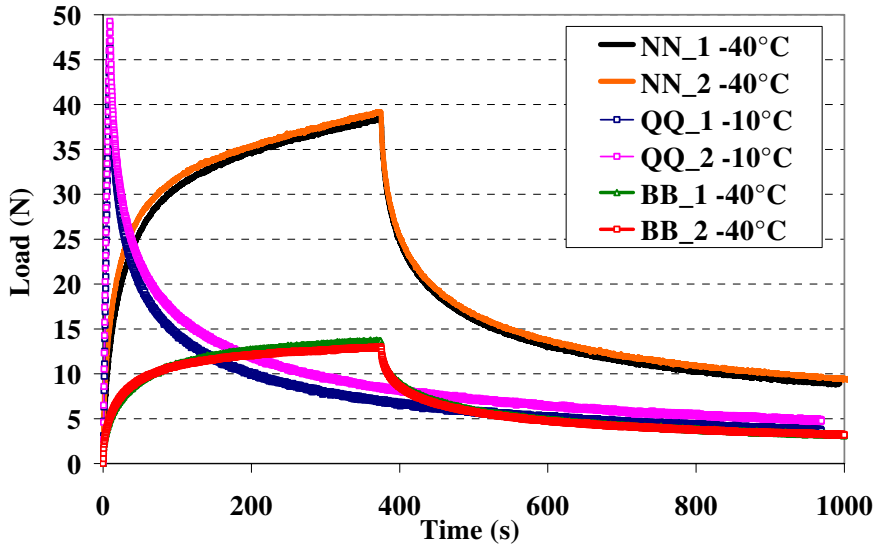


Figure 5 Stress relaxation test for sealants BB and NN at -40°C and sealant QQ at -10°C

Middle Tension Notch Fracture Test

Fracture mechanics have been widely used to characterize the fracture properties of the material by study of fracture energy, kinetic of crack growth, and molecular mechanisms. The theory behind fracture mechanics is that as a material is strained, energy is stored internally by chain extension, bond bending, or bond stretching modes (Griffith, 1921; Berry, 1961; Rosen, 1964; and Rivlin and Thomas, 1953). The energy is dissipated if bond breakage, chain slippage, or viscoelastic flow occur. Griffith (1921) showed that when the release strain energy per unit area of the crack surface exceeds the energy required to create a unit area of the surface, the surface tension (or intrinsic surface energy), a crack would propagate. The fracture parameters are calculated using a well-defined analytical function of the load at failure and the geometry of the specimen. Anderson and co-workers (2000 and 2001) have concluded that fracture

toughness provides a more definitive ranking of resistance to thermal cracking than the original SuperPave™ criteria. Based on these results and similar conclusions reached by the binder research community, an attempt was made to utilize mechanical-based fracture tests to characterize crack sealant material. A set of new molds were, therefore, developed to conduct the fracture toughness test.

The first developed mold, which was 100mm long, 6mm wide and 6mm thick, made use of a high-precision rod to induce a diamond-shaped notch during pouring of the hot-poured sealant (Figure 6). The dimension of the notch was 1mm thick and 3mm wide and the rod was inserted from the bottom of the mold and the sealant was poured into the mold. Once the sealant had cooled down to room temperature, the excessive portion of sealant was trimmed off and the whole mold was placed into the cooling bath of the direct tension machine for 5min prior to demolding. After 5min, the inserted notch was removed and the specimen was demolded. In this test, if the stress build up inside the material is slower than the stress relaxation ability of the material, the results may not reflect the true fracture properties of the material. Hence, a rapid loading rate was selected, and a strain rate of 66% per min was used. Although at such rapid loading rate, results showed that for ductile sealants failure could not be observed. These results may relate to the notch size, which was relatively thick, so no significant stress concentration around the crack tip may generate to propagate the crack.



Figure 6 Mold for preparing middle centered notched specimen of crack sealants

Consequently, a modified insert and base plate were designed as shown in Figure 7. The new developed insert, which has a thickness of 0.1mm and a width of 2mm and is embedded by a rectangular holder for easy handling, was used. The newly designed bottom plate has a build-in rectangular opening which can fit the holder of the insert. This ensured that the notch position can be identical for each test. The difficulty of using this design is that the base plate is not stable because there is a portion of the insert beyond the base plate. In addition, the level of the insert cannot be controlled accurately. This is especially important during the trimming of excessive sealant on the surface.

Therefore, the base plate was further modified to correct the aforementioned problems. As shown in Figure , the bottom plate was modified to become as a cuboids' shape in order to accommodate the space of insert. There is a special design shaft which allows controlling the vertical position of the insert. The insert has the same dimensions as in the previous design. Figure 9 and Figure 10 show typical test results of the middle tension notch specimen for sealants BB and ZZ at -40°C and -10°C, respectively. Sealant ZZ failed right after a few percents of elongation, which shows a typical brittle type of failure. However, for sealant BB, there was no failure observed even when the machine limit was reached (ε=30%). The material behaves as a ductile material, which exhibits a yield point followed by a plastic flow after the yield point. Although this fracture mechanics test has great potentials, it was not further

considered at this point because some of the sealants exhibit ductile behavior over the current testing range.

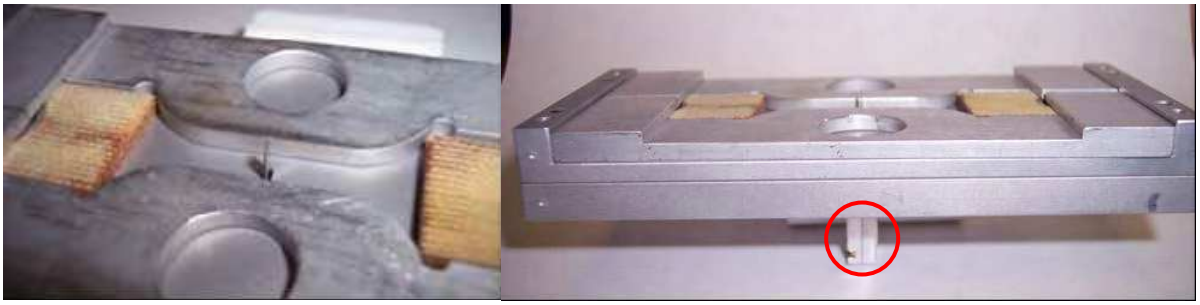


Figure 7 Improved insert with modified base plate for the middle tension notch specimen in direct tension test

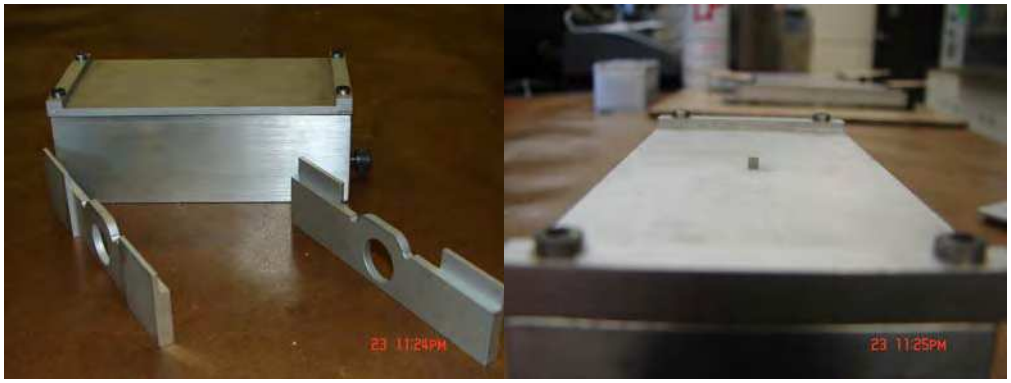


Figure 8 Newly designed mode for the middle notch tension fracture specimen. This mode allows creating a notch at a precise position in the specimen and is able to control the height of the pin for ease of trimming excessive sealant material.

Tensile Stress-Strain Test

A tension test consists of slowly pulling a specimen of crack sealant in tension until it breaks. The dog-bond shaped specimen used in the DTT has a rectangular cross section, and its ends are enlarged so that when crack sealant is poured into the mold, it would have large adhesive area between the crack sealant and end tabs. The end tabs are made from Phenolic G-10 material, to provide good bonding. The standard procedure (AASHTO TP3), with specimen preparation as modified by Ho and Zanzotto (2000), was used. The specimen was fixed at one end and pulled from the other end. The motion between the fixed and moving crossheads is controlled at a constant speed; as a result, the material is deformed under a constant strain rate. The specimen deformation is measured using a linear variable differential transducer (LVDT). In addition to deformation, the load and temperature during the test are also measured and acquired by the equipment's data acquisition system.

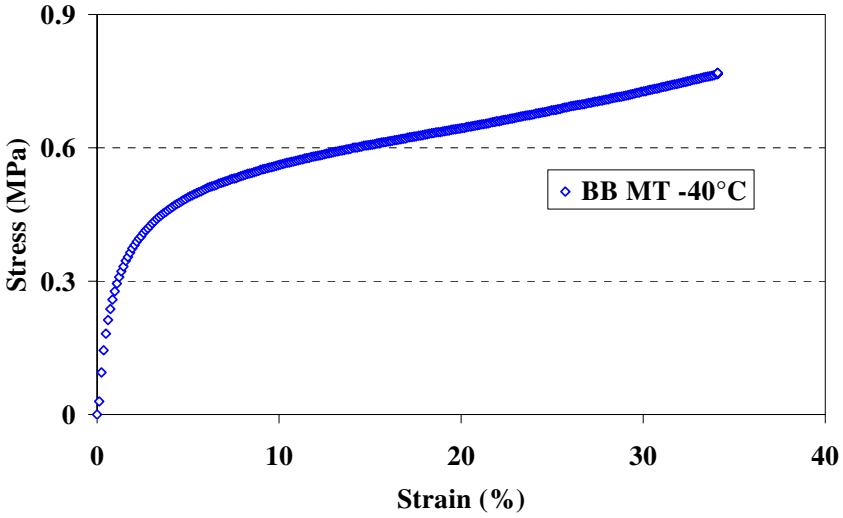


Figure 9 Middle-notched tension test for sealant BB at -40°C

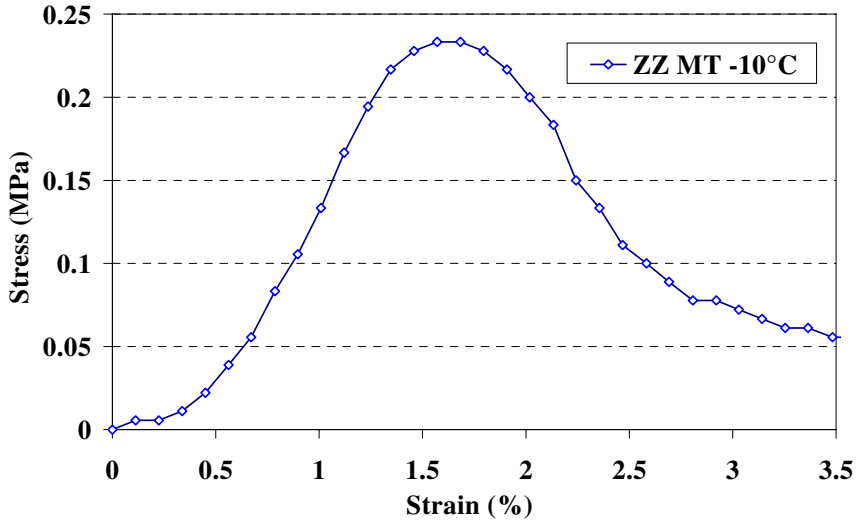


Figure 10 Middle-notched tension test for sealant ZZ at -10°C

To control the testing temperature in DTT, a fluid bath reservoir, made of stainless steel and insulated with high-density foam backing, is used. A circulating chiller allows the bath temperature to reach as low as -40°C, with a stability of +/- 0.1°C. During the test, the dog-bone specimen is pulled until rupture occurs or until the maximum traveling distance is reached. A specimen dimension of 40mm long, 6mm wide and 6mm thick with an effective gauge length of 33.8mm was used as a first trial. These dimensions are identical to the DTT specification for asphalt binders.

Six replicates of each sealant were extended at a strain rate of 3% per min for sealants BB, QQ, and NN. Sealants were tested at various low temperatures because of the variation in their composition and application location. Figure 11 shows the stress-strain relationship for six replicates of sealant QQ, which were tested at -10°C. The average stress at failure was 1.7MPa, with a COV of 14.6%. The average strain at failure was 0.7%, with a COV of 15.8%. When only the three maximum stresses at failure were considered in calculating the average stress at failure, it was 1.9MPa, with a 9.8% COV; while the average strain at failure was 0.8%, with a

COV of 13.8%. Sealant BB was tested at –40°C using six replicates, Figure 12. The extension limit was reached; but the material did not fail. The stress at 20% strain varied between approximately 0.24 and 0.28MPa.

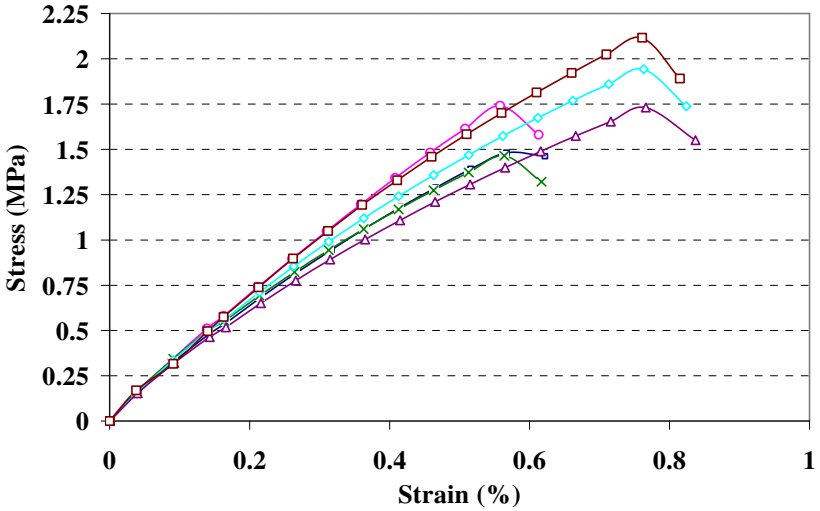


Figure 11 Stress-strain curve of sealant QQ replicates at -10℃.

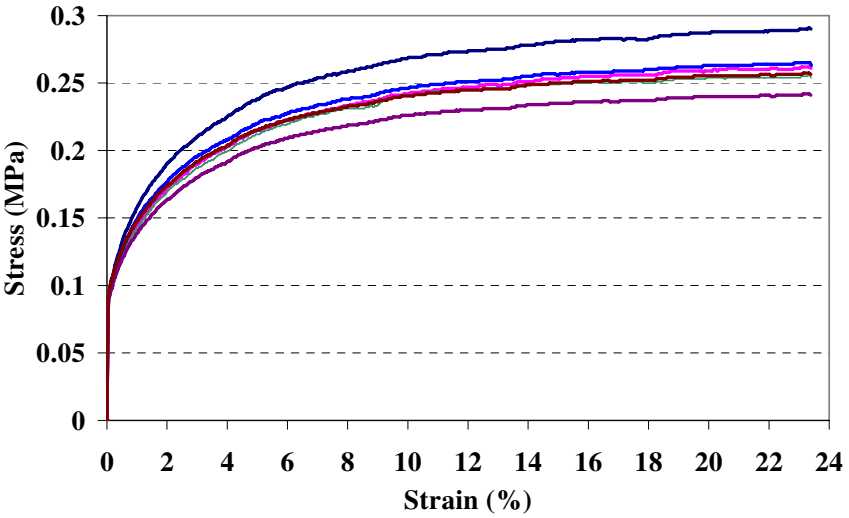


Figure 12 Stress-strain curve of sealant BB replicates at -40℃.

Sealant NN was also tested in replicates at –40°C at a strain rate of 3% per min; another set of specimens was tested at 6% per min. As shown in Figure 13, none of the specimens failed. The average stress at 20% strain for the specimens tested at 3% per min was approximately 0.9MPa. For the specimens tested at 6% per min, the average stress at 20% strain was around 1.15MPa. Even though Sealants BB and NN did not break at –40°C, Sealant BB needed less force to bring it to a 20% strain than that needed for Sealant NN. This suggests that Sealant BB is softer than Sealant NN at this temperature.

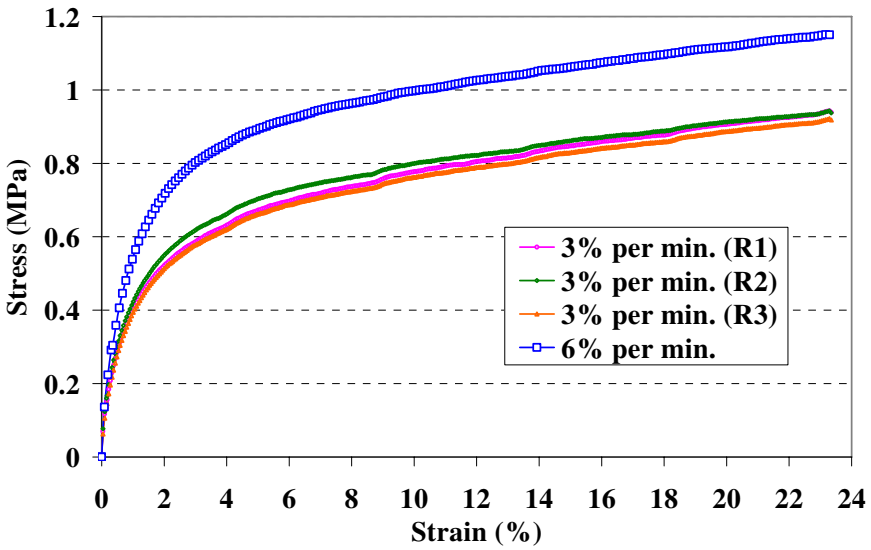


Figure 13 Stress-strain curve of sealant NN replicates at -40℃.

To find a specimen size that could be brought to failure, several specimen sizes were evaluated. The length of the specimen was varied by changing the space between the two aluminum end pieces that would fit into the clamps of the DTT. The width of the specimen was also varied using modeling clay. Figure 14 shows the mold designed for this experiment and a specimen being tested in the DTT. The smallest sample size tested was 8mm long, 6mm wide and 3mm thick. Replicates of Sealant BB were tested in these three configurations at 3% per min strain rate. Figure 15 shows the stress-strain curve; some ductile sealants did not fail. A 100% strain was achieved at approximately 0.7MPa.

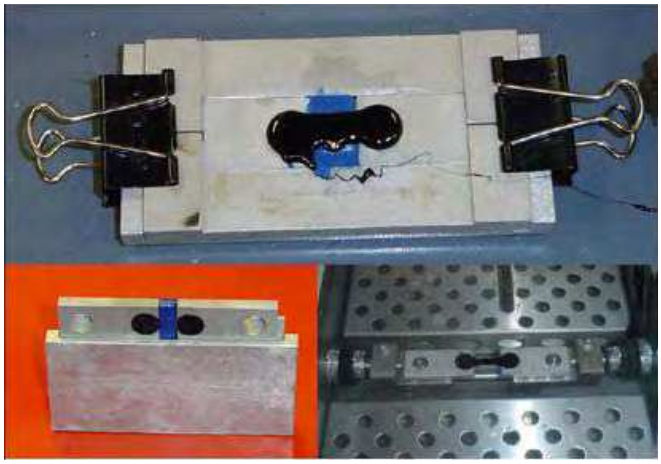


Figure 14 Specially designed mold to test small specimens in the DTT device

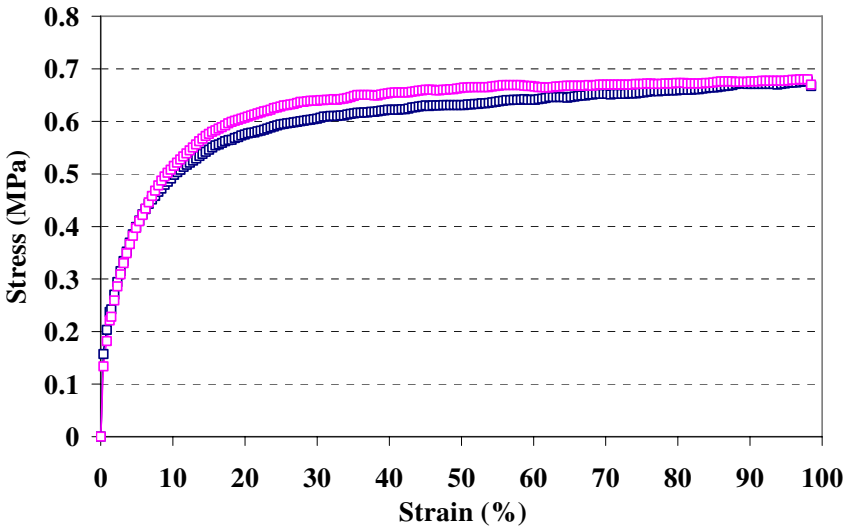


Figure 15 Stress-strain curves for sealant BB at -40°C using 8x6x3mm specimen

The preliminary tension test results show that the mechanical properties of crack sealants widely vary. Some sealants might rupture within a relatively small percent extension; while other sealants can be stretched more than 90% strain without rupture. As mentioned in the crack movement section, the opening of a crack in the winter season can vary from 10 to almost 100% compared to its opening in the summer season. The opening value depends on the geographical location and pavement type. Therefore, the experimental effort has aimed to develop a specimen geometry that would allow the specimen to extent more than 90%.

The current SuperPave™ DTT test specimen (Figure 16) has an effective gauge length of 33.8mm (Bouldin et al., 1999) and a limited allowable traveling distance. The maximum extension that could be reached is 30%. Therefore, a shorter effective length specimen is needed. In addition to the length modification, the thickness of the specimen was also modified. The reason is some sealants, which contain crumb rubbers as fillers, were difficult to pour in the SuperPave™ DTT mold (6mm). The particle size of the crumb rubber can be as large as 1.2mm (Georgia DOT); therefore, when this type of sealant is used, the bottom corner of the mold may not be completely filled. Hence, in this study, the effort aimed to optimize the specimen thickness, which facilitates sealant pouring while achieving an effective gauge length that can increase the level of extension.

To examine the feasibility of using a smaller specimen size, a finite element (FE) analysis was conducted to determine an optimal size and to simulate crack sealant behavior. The optimal specimen size must meet two criteria: uniform stress distribution within the specimen web as well as ease of specimen preparation. In the FE analysis, 10 specimen sizes were evaluated. Various dimensions for the specimen total length, web length, and flange length and width were proposed (Table 5). The dimensions were selected to investigate the effect of specimen's thickness and width simultaneously. Each specimen was fixed at the lower end of the flange and a deformation rate was applied at the other upper end of flange at 1mm/min as shown in Figure 17. Results of the FE quasi-static analysis were obtained and the tensile stress distribution for each specimen's geometry was determined as shown in Figure 18. Specimen g was selected for this study

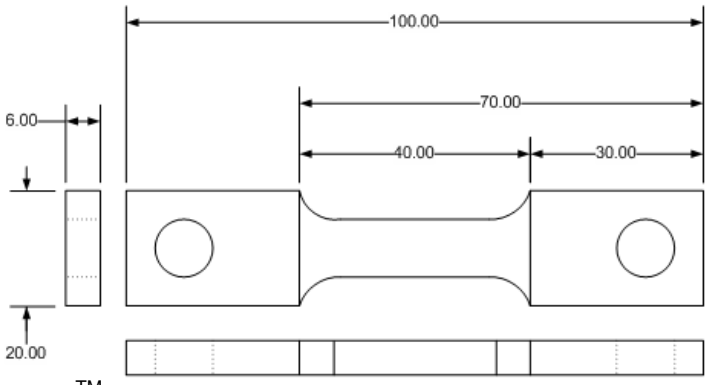
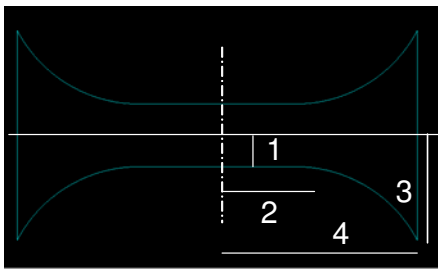


Figure 16. SuperPave™ binder specimen geometry specification for DTT (units are in mm).

Table 5 Trial Dimensions for the CSDTT Specimens (in mm)

Specimen	1	2	3	4
a	3	8	10	19
b	2.75	8	9.5	19
c	2.75	8	9.5	18
d	2.75	6	9.5	15
e	2.5	6	8	12
f	2.5	6	8	12
g	3	6	7	12
h	2.75	6	7	10
i	3	6	6	10
j	3	6	5	10



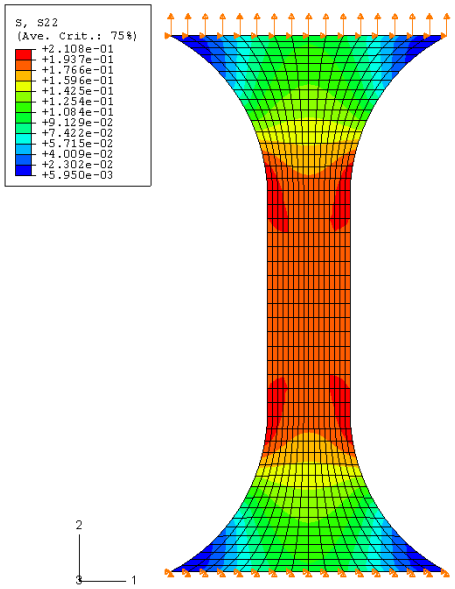


Figure 17 2-D finite element model for the CSDTT specimen

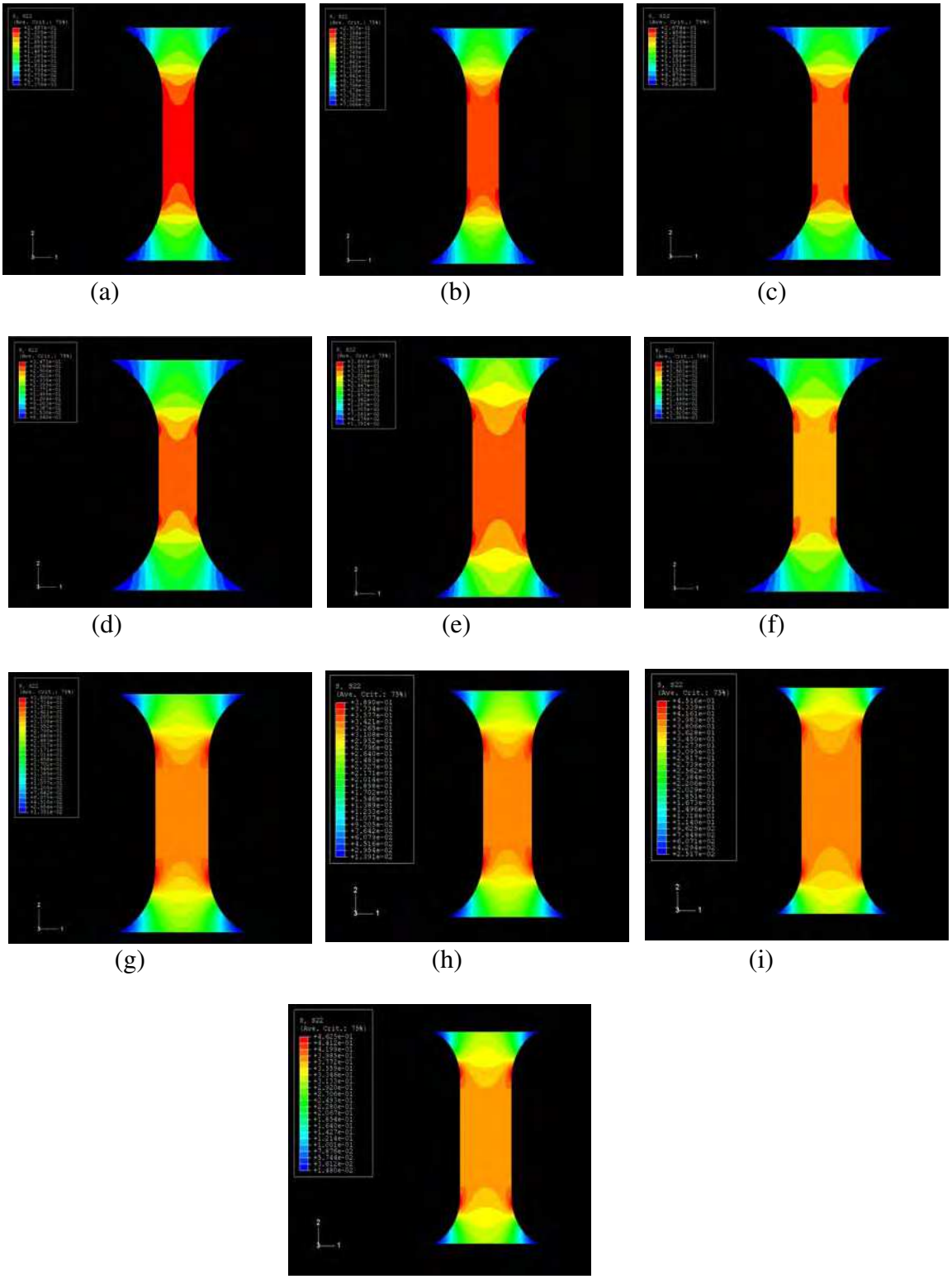


Figure 18 Stress distribution within various sizes of DTT specimens

The new specimen was determined to be 24mm long, 6mm wide and 3mm thick with an effective gauge length of 20.3mm. The maximum extension can be achieved using this

specimen is 19mm, which is equivalent to approximately 94% strain. Table 6 presents the comparison of the SuperPave™ binder DTT specimen geometry to the one used in this study. Appendix B describes the determination of the effective gauge length of the new specimen, using finite element analysis. Experimentally, the effect of specimen size and geometry is discussed later in the report.

In summary, although the tension stress-strain is not the simplest test as of the four basic properties (stress, strain, rate of deformation, and temperature) only temperature can be kept constant, it was selected because it simulates field loading of crack sealant when extended. In addition, the relatively short testing time makes it suitable as a specification test.

Table 6 Comparison of direct tension specimen dimensions

Specimen Type	Width (mm)	Thickness (mm)	Nominal Length (mm)	Effective Length (mm)
SuperPave™	6	6	40	33.8
Crack Sealant	6	3	24	20.2

Test Procedure

The procedure used in this study mainly follows the procedure proposed for SuperPave™ binder testing (AASHTO TP3), except an improved sample preparation procedure suggested by Ho and Zanzotto (2000) was adopted. The sealant is heated to the manufacturer's recommended installation temperature for 30min, and then firmly stirred before pouring into a dog-bone shaped aluminum mold. The mold and ceramic tile were placed into separate oven, which was preheated to 50°C lower than the manufacturer's recommended pouring temperature, 15min prior to pouring the sealant into the mold. Using a temperature that is 50°C lower than installation temperature is based on research conducted by Masson et al. (2006), who reported a 50°C drop while the sealant was in contact with the crack wall right after pouring. Using this method, the sealant is maintained in a liquid state after it comes into contact with the mold to keep it homogeneous and workable during sample preparation. The specimen is then allowed to cool to room temperature for one hour. It is then placed in the environmental control chamber for 5min, and then de-molded. The specimen was next placed in the fluid bath to condition for one hour at testing temperature before the test was performed.

The tension stress-strain test was designed to apply a constant strain rate of 6% per min to a specimen, which is equivalent to the 1.2mm/min for the CSDTT specimen geometry. The maximum travel distance of the DT device for the CSDTT specimen is 19mm; therefore, the CSDTT specimen can reach approximately 95% strain in 15min. Figure 19 shows the loading and deformation results for sealant BB at -40ºC.

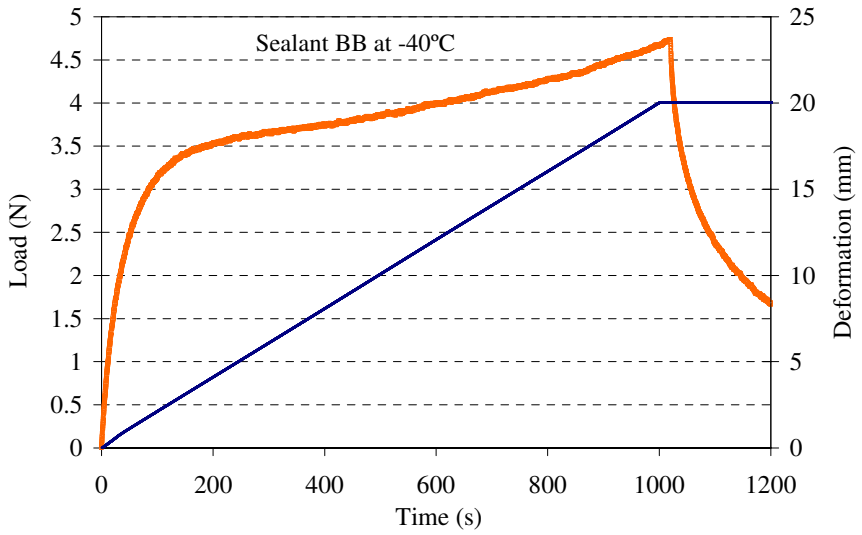


Figure 19 The orange curve represents the loading loci and the blue curve shows the deformation loci for CSDTT specimen of sealant BB at -40ºC at a strain rate at 1.2mm/min

Performance Parameters

True Stress and Strain

In the SuperPave ™ binder specification, the parameters reported at the failure point are the engineering stress and strain. The strain at failure is defined at the maximum stress when the specimen fractures. When the specimen does not fracture, the stress-strain value at 10% strain is reported and note as "greater than 10%". For the crack sealant, true stress and strain are reported instead of engineering stress and strain. In addition to the stress-strain at failure, two addition parameters are recorded and reported for the crack sealant: strain energy density and percent modulus decay.

Determining the stress-strain at failure from DTT is clear for brittle or brittle-ductile behaviors, as in DTT for binders. However, if this test is conducted on a very soft material such as some crack sealants, the sample may exhibit large strain before failure. Hence, the maximum load may be difficult to determine. In this case, calculating the stress and strain as presented by Equations (1) and (2) is no longer valid. The reduction in the cross-sectional area is significant and must be considered in the calculation. Therefore, the true stress and true strain of the tension test should be considered.

The stress and strain calculated in Equations (1) and (2) usually refer to the engineering stress and engineering strain. The engineering stress is obtained by dividing the load by the original cross-section area. The SuperPave™ binder specification system has limited the minimum allowable strain to be 1% and stop the test at strain of 10% (Anderson et al., 1994). In this case, the error between engineering and true stress is about 10^{-4}, which is negligible. For materials that exhibit large deformations during the course of this test, it is essential to use the concept of true stress and true strain in the calculation. Finite changes in area and length are considered in the determination of true stresses and strains. True stress is simply calculated as dividing the load, P, by the current cross-sectional area, A_i, rather than the original area A_0:

$$\tilde{\sigma} = \frac{P}{A_i} \qquad (3)$$

where,

$\tilde{\sigma}$ = true stress; and
A_i = current cross-section area.

For materials that behave in a ductile manner, once the strains have increased substantially beyond the yield region, most of the strain that has accumulated is inelastic strain. Since plastic strain or creep strain are mainly contributed by re-orientation of the molecular chain therefore, neither of them contributes to volume change, the volume change in a tension test is limited to small amount associated with elastic strain. Thus, it is reasonable to approximate the volume as constant. For that reason, the volume conservation assumption can be applied. The current area A_i subsequently can be calculated from the true strain (total volume = $A_0L_0=A_iL_i$; Dowling, 1999):

$$\tilde{\varepsilon} = \ln\left(\frac{A_0}{A_i}\right) \tag{4}$$

In the DTT (Equation 5), a constant tensile true strain rate $\dot{\varepsilon}$ is applied; therefore, it can relate A_i to the initial area of cross-section A_0:

$$A_i = A_0 \times e^{(-\dot{\varepsilon} t)} \tag{5}$$

Therefore, the true tensile stress can be given as follows:

$$\tilde{\sigma} = \frac{P}{A_i} = \frac{P \times e^{(\dot{\varepsilon} t)}}{A_0} \tag{6}$$

The failure stress and strain are calculated as true stress and true strain for crack sealant materials. The failure strain for crack sealant in DTT is considered at the maximum stress if the material fractures in the brittle state. In this case, the difference between true stress and engineering stress is insignificant. If the material fails in the brittle-ductile transition, the failure strain is identified at the point of maximum stress. If the material does not fail/rupture due to a ductile behavior, the strain at failure is identified at the 90% strain extension.

Strain Energy Density

Toughness is measured by the area under the stress-strain curve. This area has the units of energy per unit volume and is the work expended in deforming the material. The deformation may be elastic, recoverable, or permanent (irreversible deformation). The toughness is selected as a parameter because a sealant is rarely stressed in the field to immediate fracture. In this case, strain energy density for crack sealant could be meaningful parameter.

Percentage Modulus Decay

Relaxation modulus is considered a fundamental property of the viscoelastic material. Bituminous crack sealant is a typical viscoelastic material, which exhibits both elastic (solid-like) and viscous (fluid-like) mechanical behavior. A straightforward method to obtain the relaxation modulus of a viscoelastic material is to conduct a stress relaxation test. This test, which is shown in Figure 4, consists of applying an instantaneous step deformation to the material and the reduction of load is measured. The relaxation modulus can then be calculated, as follows:

$$E(t) = \frac{\sigma(t)}{\hat{\varepsilon}} \tag{7}$$

where,

E(t) = stress relaxation modulus function ;
$\sigma(t)$ = stress measured as a function of time (t); and
$\hat{\varepsilon}$ = constant step strain applied instantaneously.

However, this test may not be applicable for crack sealant materials because of two reasons: First, due to rapid stretching, most sealants exhibit adhesive failure between the end tabs and the sealant interface than in the sealant itself; second, the stretched length varied from a sealant to another. There is no unique stretch length that could be used for all tested sealants; hence, from a specification test point of view, this is unacceptable.

Instead of conducting a stress relaxation test to obtain the relaxation modulus function, the modulus may be estimated using the tension stress-strain test. In the SuperPave ^{TM} DTT, the relaxation modulus is calculated simply by dividing the instantaneous stress by the strain and by fitting a second order polynomial function, which is then converted into relaxation modulus (Smith, 1976). Marasteanu (2000) used this approach to convert the binder DTT data to relaxation modulus and concluded that the strain rate could affect the DTT data. He suggested that this conversion could only be valid if the test was performed within the linear viscoelastic region. The approach was used with the crack sealant direct tension data; however, the data did not fit the second order polynomial for some sealants. This could be due to the high level of extension. Another approach to obtain the relaxation modulus from the test data is using three terms Prony series. From the *Boltzman superposition principle*, the stress-strain relationship for a viscoelastic material can be expressed as follows:

$$\sigma(t) = \int_0^t E(t-t') \frac{d\varepsilon(t')}{dt'} dt' \tag{8}$$

where,

$\sigma(t)$ = stress history;
$\varepsilon(t)$ = strain history; and
E(t) = relaxation modulus.

A mechanical analog, which includes discrete elastic (spring) and viscous elements (dashpot), Figure 22, is usually used to link the input strain and output stress. Therefore, the relaxation function can be simulated as various combinations of spring and dashpot elements. Of these two basic elements, various models (e.g., Maxwell and Kelvin elements) can be built to describe the viscoelastic response of the material to a given excitation. To describe the isotropic viscoelastic behavior of hot-poured crack sealants, a generalized Kelvin-Voigt model, which consists of a spring and dashpot connected in series, was selected in this analysis. In the case of a viscoelastic solid, the relaxation modulus at a time t using Generalized Kelvin model can be expressed as follows:

$$E(t) = E_0 - \sum_{i=1}^{K} E_i (1 - e^{-t/\tau_i}) \tag{9}$$

where,

E(t) = the relaxation modulus at time t;
E_i = material constants; and
τ_i = retardation times.

Equation (9) is also known as a Prony series expansion, and it represents a series of decaying exponentials. Upon application of a strain, the individual spring placed at the start of the chain (first term in Equation [9]) responds instantly. In contrast, the spring and the dashpot of the different Kelvin elements exhibit constrained motions as they are restrained from experiencing the same strain at any given time. The retardation times are generally used to provide an indication of the amount of time required for a certain component of the material (e.g., polymer) to respond to the imposed creep load. Each retardation time contributes to the fitting of the model in one order of time magnitude and is associated with a component of the material responding to the load. The number of terms in the Prony series should not be greater than the number of logarithmic decades covered by the span of the test. For example, if a creep test is conducted for 1000s, the number of Prony series terms should not exceed three.

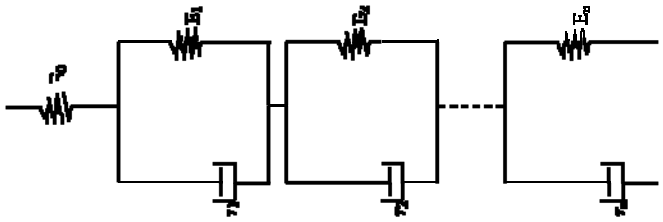


Figure 20. Mechanical representation of a Prony series to describe a viscoelastic solid.

Substituting Equation (9) into Equation (8), the following expression of the stress results:

$$\sigma(t) = E_0\varepsilon(t) - \int_0^t \sum_i^N E_i(1 - e^{\frac{-(t-t')}{\tau_i}}) \frac{d\varepsilon(t')}{dt'} dt' \quad . \qquad (10)$$

In the DT test, sealant is subjected to a constant strain rate beginning at time zero, $\varepsilon(t) = \begin{Bmatrix} 0 \ \ for\, t < 0 \\ Rt \ for\, t \geq 0 \end{Bmatrix}$, with R as the strain rate. The above convolution integral can then be solved as follows:

$$\sigma(t) = E_0\varepsilon(t) - \sum_i^N E_i\dot{\varepsilon}\left[t - \tau_i\left(1 - e^{\frac{-t}{\tau_i}}\right)\right] \qquad (11)$$

Equation (11) shows that the stress can be expressed as a function of time (t) and applied strain rate ($\dot{\varepsilon}$). The equation is used to fit the experimental data by means of the least squares (LS) technique to obtain the material constants E_0, E_i, and τ_i. This analysis has shown that a three-term Prony series (N=3) can provide good fitting results from the experimental data since the testing time is usually less than 1000s. An Excel Visual Basic template has been designed to obtain the fitting parameters. A typical fitting of the model to the experimental stress data is shown in Figure 21. The relaxation modulus function (E[t]) can then be plotted in logarithm scale (Figure 22).

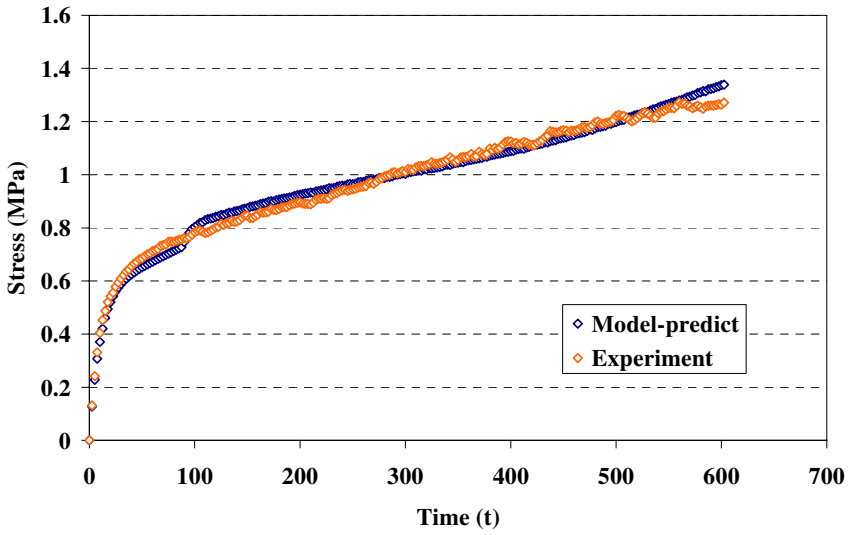


Figure 21 Fitting the experimental stress data to the proposed 2-term Prony series model

Once the relaxation function of the tested sealant is obtained, it can be used to evaluate the sealant's stress relaxation ability. The greater the percentage of modulus decay means the smaller the amount of stress that remains inside the sealant. Therefore, the percentage modulus decay after time t of loading is calculated as follows:

$$M_r(t) = \frac{E(t) - E(0)}{E(0)} \qquad (12)$$

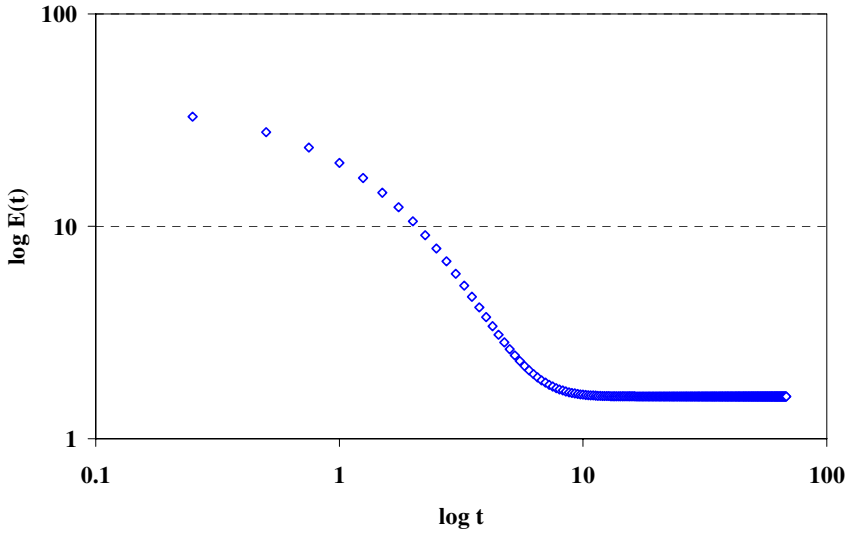


Figure 22 Relaxation modulus function plotted in logarithm scale

RESULTS AND DISCUSSION

The function of crack sealant is very different from that of asphalt binder. Asphalt binder acts as a glue to hold the aggregate together in the pavement, and provides a portion of the pavement's structural capacity. Therefore, the strength of the asphalt binder is an important factor. On the contrary, crack sealant does not provide any structural contribution to the pavement system. The most important properties of crack sealant at low temperature are extendibility and load relaxation ability. These two properties can ensure that a sealant properly dissipates the imposed loading when a crack opens and does not rupture. Therefore, stress relaxation and strain extension capabilities of the sealant are the most important parameters for its successful application.

Extendibility

The extendibility of 15 crack sealants tested under various temperatures was measured (Table 7). Four replicates of each sealant under each temperature were tested and three test results, which gave the best coefficient of variance (COV), were reported. As shown in Table 7, the stress and strain at 90% extension or at the point of rupture and their average value and COV are reported. If the material fails/ruptures in the brittle-ductile transition, the failure strain is identified at the point of the maximum stress. If the material does not fail/rupture as it exhibits ductile behavior, the strain at failure is identified at the 90% strain extension.

All the sealants were tested at their recommended lowest service temperature and if the sealant could not pass at that temperature, it was tested at +6°C. The results show that five out of the 15 tested sealants can be stretched to more than 90% strain at the selected testing temperatures: Sealants BB and PP at -40°C, sealants NN and AE at -34°C, and sealant MM at -28°C. However, sealants QQ, YY, ZZ, and AB could not be stretched to 90% strain at the selected testing temperature.

The data in Table 7 were also used to evaluate test repeatability. Overall, the test results were repeatable. The lowest COV for the strain was 0.78% for sealant YY tested at -4°C. The highest COV was 15.3% for sealant UU at -22°C. The lowest peak/failure stress COV for stress was 1.3% for sealant BB tested at -40°C; and the highest COV for peak/failure stress was 11.5% for sealant UU at -10°C. In general, a sealant having high extendibility and low stress would be expected to perform better in the field at low temperature. The peak stresses for the tested 15 sealants are reported in Table 8.

Table 7 Extendibility for 15 Sealants at Various Temperatures

Sealant	Temp	Extendibility				
	(°C)	(%)				
		Rep. 1	Rep. 2	Rep. 3	Avg.	COV (%)
QQ	-4	0.94	1.01	0.95	0.97	4.05
	-10	0.35	0.37	0.31	0.34	8.86
EE	-4	32.46	31.74	31.94	32.05	1.15
	-10	26.49	24.86	25.64	25.66	3.18
	-16	2.30	2.55	2.19	2.35	7.83
ZZ	-4	34.94	32.20	29.41	32.19	8.59
	-10	2.64	2.62	2.37	2.54	5.72
	-16	1.06	1.01	1.13	1.07	5.81
YY	-4	14.11	14.04	13.90	14.02	0.78
	-10	2.88	2.48	2.88	2.74	8.40
	-16	1.90	1.67	1.51	1.69	11.59
AB	-10	2.68	2.91	2.50	2.70	7.54
	-16	1.77	1.95	1.76	1.83	5.90
VV	-16	3.35	4.19	3.97	3.84	11.33
	-22	0.59	0.59	0.51	0.57	8.50
UU	-10	32.14	32.96	31.21	32.10	2.73
	-16	26.36	22.46	23.95	24.26	8.12
	-22	14.59	19.78	16.74	17.03	15.31
DD	-22	90+	90+	90+	90+	N/A
	-28	80.77	85.55	83.20	83.17	2.87
	-34	12.00	15.44	14.65	14.03	12.85
AE	-40	90+	90+	90+	90+	N/A
MM	-28	90+	90+	90+	90+	N/A
	-34	90+	90+	90+	90+	N/A
	-40	4.54	5.40	5.70	5.21	11.58
WW	-34	90+	90+	90+	90+	N/A
	-40	0.51	0.63	0.55	0.56	10.94
NN	-34	90+	90+	90+	90+	N/A
	-40	49.15	46.50	52.48	49.38	6.07
AD	-40	90+	90+	90+	90+	N/A
PP	-34	90+	90+	90+	90+	N/A
	-40	22.31	17.81	18.18	19.43	12.86
BB	-40	90+	90+	90+	90+	N/A

Table 8 Peak Stress for 15 Sealants at Various Temperatures

Sealant	Temp (°C)	Peak Stress MPa				
		Rep. 1	Rep. 2	Rep. 3	Avg.	COV (%)
QQ	-4	1.05	1.06	1.23	1.11	9.09
	-10	0.8	0.85	0.78	0.81	4.45
EE	-4	0.79	0.61	0.65	0.68	13.83
	-10	0.88	0.92	0.87	0.89	2.97
	-16	1.56	1.52	1.61	1.56	2.88
ZZ	-4	0.78	0.66	0.73	0.72	8.33
	-10	0.74	0.69	0.65	0.69	6.50
	-16	0.82	0.78	0.87	0.82	5.48
YY	-4	0.46	0.46	0.42	0.45	5.17
	-10	0.64	0.57	0.64	0.62	6.55
	-16	1.87	1.65	1.9	1.81	7.56
AB	-10	0.3	0.27	0.24	0.27	11.11
	-16	0.3	0.32	0.3	0.31	3.77
VV	-16	1.12	1.25	1.18	1.18	5.50
	-22	0.7	0.69	0.6	0.66	8.30
UU	-10	0.31	0.35	0.39	0.35	11.43
	-16	0.67	0.68	0.73	0.69	4.64
	-22	1.34	1.23	1.29	1.29	4.28
DD	-22	0.46	0.45	0.45	0.45	1.27
	-28	1.27	1.49	1.31	1.36	8.64
	-34	1.39	1.59	1.42	1.47	7.35
AE	-40	2.77	2.53	2.45	2.58	6.45
MM	-28	1.45	1.75	1.55	1.58	9.65
	-34	1.12	1.16	1.25	1.18	5.66
	-40	2.59	2.73	2.91	2.74	5.85
WW	-34	0.82	0.81	0.77	0.80	3.31
	-40	2.43	2.22	2.17	2.27	6.07
NN	-34	1.09	1.06	1.05	1.07	1.95
	-40	1.85	1.73	1.9	1.83	4.78
AD	-40	1.9	1.86	1.81	1.86	2.43
PP	-34	0.46	0.48	0.51	0.48	5.21
	-40	1.2	1.13	1.23	1.19	4.32
BB	-40	0.99	1	1.02	1.00	1.52

Strain Energy Density (SED)

Strain energy density (SED) is calculated as the area under the stress-strain curve. It is the work expended in deforming the material, and it has the units of energy per unit volume. Two sealants can fail or reach a similar stress-strain point; but have a very different SED value. In addition, a sealant may have the same SED at different temperatures. Therefore, it is

recommended to use SED with extendibility. It is desirable to have a high SED and a high extendibility in the field. The SED results for the 15 sealants are presented in Table 9.

Table 9 SED Results for Nine Sealants at Various Temperatures

Sealant	Temp	SED				
	(°C)	Rep. 1	Rep. 2	Rep. 3	Avg.	COV (%)
QQ	-4	5.2E-03	5.8E-03	6.2E-03	5.7E-03	8.6
ZZ	–4	2.2E-01	1.6E-01	1.6E-01	1.8E-01	0.1
	–10	1.3E-02	1.2E-02	9.5E-03	1.1E-02	4.0
	-16	5.1E-03	4.7E-03	5.8E-03	5.2E-03	9.9
YY	–4	4.8E-02	4.6E-02	4.4E-02	4.6E-02	5.0
	–10	1.2E-02	8.9E-03	1.2E-02	1.1E-02	0.0
	-16	1.5E-02	1.7E-02	1.5E-02	1.6E-02	7.1
AB	-10	3.5E-03	3.8E-03	6.4E-03	4.5E-03	4.0
	-16	2.6E-03	2.3E-03	2.1E-03	2.3E-03	9.1
EE	-4	1.5E-01	1.6E-01	1.6E-01	1.5E-01	5.8
	-10	1.7E-01	1.8E-01	1.8E-01	1.8E-01	3.4
	-16	3.8E-02	2.9E-02	2.6E-02	3.1E-02	19.4
VV	-22	2.3E-03	1.6E-03	2.3E-03	2.1E-03	0.1
	-16	2.2E-02	2.0E-02	1.9E-02	2.0E-02	6.4
UU	-10	8.7E-02	1.0E-01	1.0E-01	9.8E-02	9.2
	-16	1.5E-01	1.9E-01	1.6E-01	1.7E-01	13.1
	-22	4.0E-02	3.3E-02	3.8E-02	3.7E-02	10.1
DD	-22	3.8E-01	3.7E-01	3.2E-01	3.6E-01	8.9
	-28	3.4E-01	3.2E-01	3.1E-01	3.2E-01	5.2
	-34	6.3E-02	4.8E-02	5.5E-02	5.5E-02	13.1
AE	-40	1.6E+00	1.4E+00	1.5E+00	1.5E+00	7.8
MM	-34	1.1E+00	9.8E-01	1.1E+00	1.1E+00	6.1
	-40	7.1E-02	6.4E-02	7.4E-02	7.0E-02	7.8
WW	-34	7.8E-01	7.2E-01	8.1E-01	7.7E-01	6.0
	-40	5.4E-03	6.1E-03	5.8E-03	5.7E-03	5.7
NN	-34	7.5E-01	7.2E-01	7.1E-01	7.3E-01	2.3
	-40	7.4E-01	7.1E-01	7.6E-01	7.4E-01	3.4
AD	-40	1.3E+00	1.2E+00	1.2E+00	1.2E+00	3.7
PP	-34	8.1E-02	8.9E-02	1.0E-01	9.0E-02	11.1
	-40	8.6E-02	6.9E-02	7.6E-02	7.7E-02	11.1
BB	-40	2.1E-01	1.9E-01	2.4E-01	2.1E-01	10.5

Modulus Decay Percentage

The percent modulus decay after 10s of loading for the 15 tested sealants was calculated at various testing temperatures (Figure 23 and 26). As expected, the percent modulus decay increased with the increase in the testing temperature. Sealant QQ at -4 and -10°C, ZZ at -16°, VV at -22°C, and WW at -40°C resulted in zero percent modulus decay. This could be due to either the tested specimen failed within 10s or the elastic behavior of the material; hence no modulus reduction occurred prior to failure. Sealant AB in Figure 23 shows

an opposite trend in the percentage of modulus decay. This could be to the quality of data fitting since the calculation of percent modulus decay heavily relies on fitting the experimental data with viscoelastic material model (Prony series). Sealant AB failed at 2.7% and 1.83% strain at -10 and -16°C, respectively and non-brittle failure were observed at both testing temperature. Material softening was observed prior specimen failure. However, the model was found to be insensitive enough to capture the softening phenomena. Therefore, the prediction percent modulus decay for such material may not accurate.

The percent modulus decay can indirectly reveal information on the material state. If the percent modulus decay at two consecutive testing temperatures is close, the material could be in the rubbery plateau state. However, if the percent modulus decay changes dramatically between two consecutive temperatures, the material could be changing between glassy transition and rubbery plateau states. This could help in the crack sealant selection process as maintaining crack sealant in the rubbery state is greatly desired.

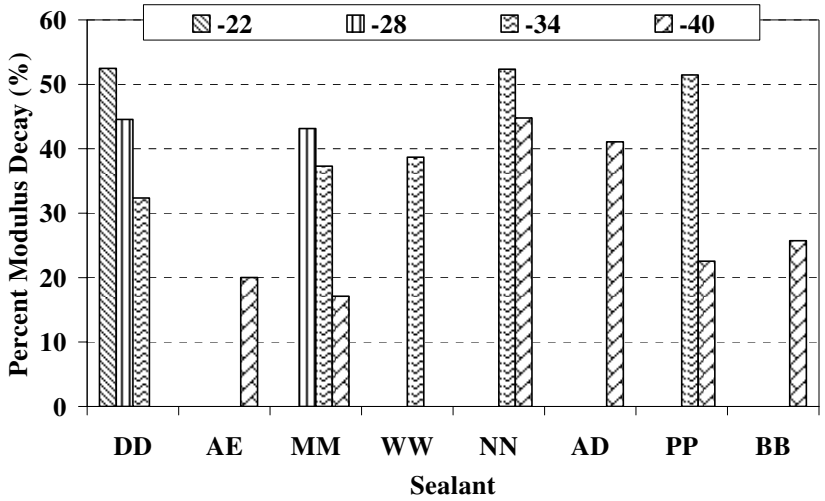


Figure 23 Percent modulus decay after 10s of loading for sealants QQ, EE, ZZ, YY, AB, VV, and UU

DISCUSSION

Crack sealant and binder are both bituminous-based material; however, crack sealant behaves as polymer modified binder. The polymer contents of crack sealant are varied from as low as 1% to as high as 18% depending on the geographical location of sealant application. Because of the high polymer content and addictives, a wider range of stress-strain behavior could be expected for crack sealants compared to asphalt binders. Four typical types of stress-strain curves of crack sealant are shown in Figure 25. Sealant may behave as a brittle plastic for which the stress-strain curve is linear until fracture with a little percentage elongation (curve A). Low polymer content and high crumb rubber modified sealant behaves this way. A brittle-ductile failure may be observed; when the tensile load reaches a maximum, sealant may fracture, curve B, or the specimen may continue to stretch after the maximum load, curve C (Figure 25). Sealant may also experience ductile failure (curves D and E). Typically, this type of sealant exhibits a yield point, followed by extensive elongation at almost constant stress. This is called the plastic flow region and is clearly a region of nonlinear viscoelasticity. After the plastic flow region, sealant may exhibit strain hardening. This type of sealant usually has relatively high polymer concentration.

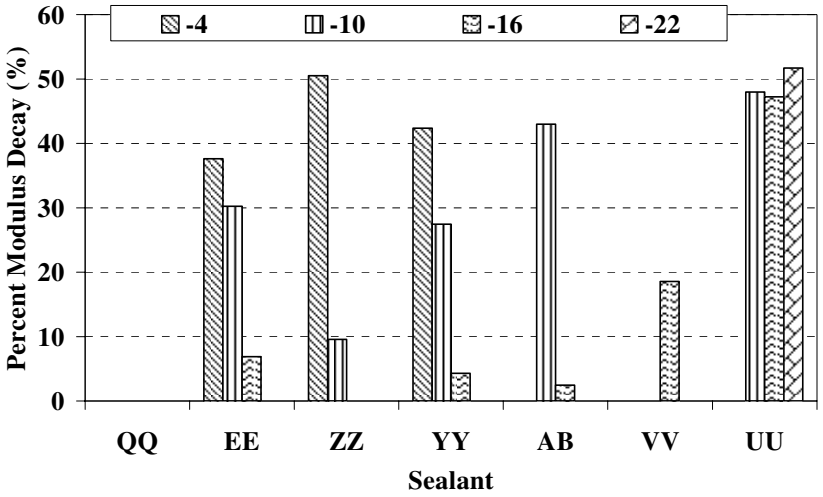


Figure 24 Percent modulus decay after 10s of loading for sealants DD, AE, MM, WW, NN, AD, PP, and BB

Sensitivity Analysis of Specimen Geometry and Loading Rate on Stress-Strain Response

Al-Qadi et al. (2007) conducted a sensitivity analysis on the specimen geometry. Three specimen geometry sizes were compared (Table 10): Type A, which is the original specimen adopted in the SuperPave™ binder specifications; Type B, which is 40mm long with an effective length of 33.8mm, 6mm wide, and 3mm thick; and Type C, which is 24mm long with an effective length of 7.5mm, 6mm wide, and 3mm thick. The effect of cross-section area can be compared using Type A and Type B specimens. Type B and Type C specimens can be used to compare the length effect. A thinner specimen, 3-mm-deep, provides better pouring control. This results in a homogeneous specimen having a strong bond with the end tabs. In addition, a shorter specimen allows higher testing elongation, close to 100% strain.

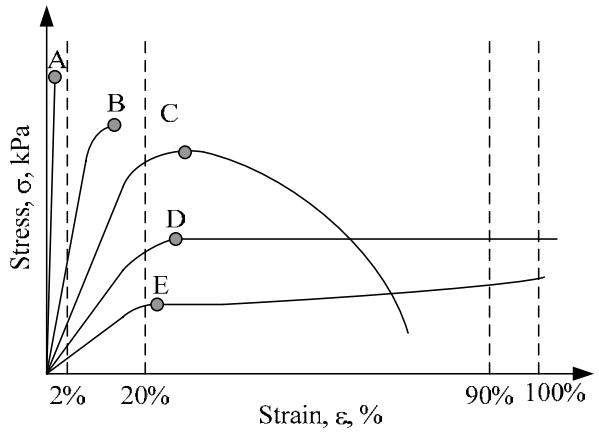


Figure 25 Stress-strain behavior of crack sealant observed in the direct tension test

Table 10 Evaluated DTT Specimen Dimensions

Specimen Type	Width (mm)	Thickness (mm)	Nominal Length (mm)	Effective Length (mm)
A	6	6	40	33.8
B	6	3	40	33.8
C	6	3	24	20.3

Crack sealant is a rate-dependent material. A common way to determine the proper loading rate for testing is by applying various loading rates and plotting the stress-strain response curves. The elongation rates used in the study were the following: 0.6, 1.5, 3.0, 4.5, and 6.0mm/min for types A and B specimens. However, an elongation rate of 1.8mm/min was used for type C specimen. It has to be noted that the deformation rates used in this study are high compared to the field-measured rates. The DT machine becomes instable at a very low loading rate. The lowest possible extension rate of the current DT machine is 0.01mm/min. In addition, it is not practical to select a test rate that is identical to the rate in the field because the test period for each specimen will be too long. Conducting the test at a high loading rate simulate greater critical conditions.

Effect of Cross-Section on Stress-Strain Response

The effect of cross-section areas on the stress-strain relationship was investigated by comparing the results obtained from testing Type A (6mmx6mm) and Type B (3mmx6mm) specimens using high-polymer-content sealants. As illustrated in Figure 26, high-polymer-content sealants, WW and PP, showed no major effects due to changes in specimen cross-section area.

Effect of Specimen Length on Stress-Strain Response

The effect of specimen length on stress-strain response for types B and C specimens was investigated (Figure 27a and b). Utilizing the same elongation rate for both types resulted in a greater stress response in the C specimen than in the B specimen. Since it is of interest to compare the stress response at the same strain level, two elongation rates, 3mm/min and 1.8mm/min, were applied to specimens B and C, respectively. Considering the corresponding specimen length, the variation in elongation rates resulted in an identical strain rate of 8.8% per min for each type.

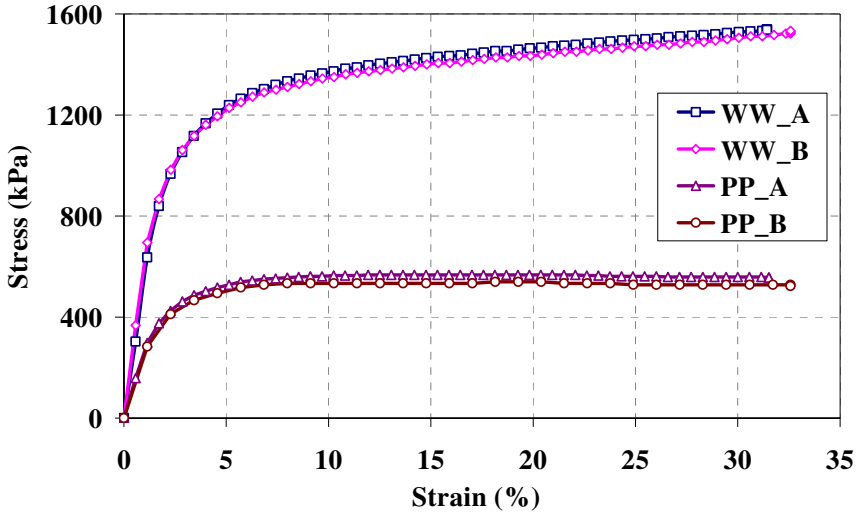
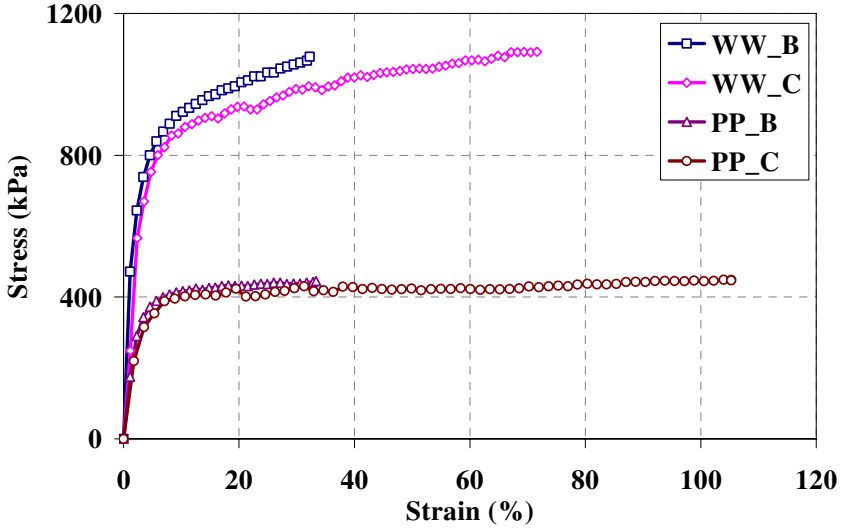
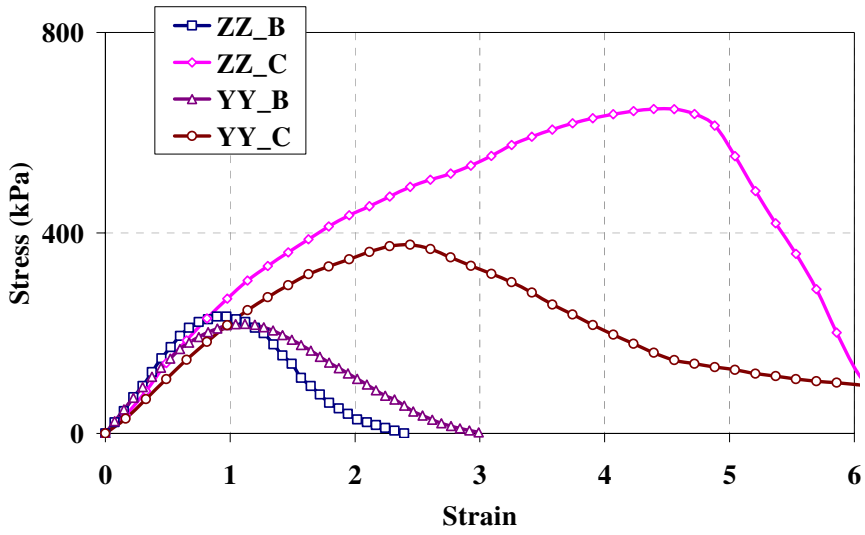


Figure 26 Effect of cross-section area on stress-strain relationship for two high-polymer-content sealants at 4.5mm/min



(a)



(b)

Figure 27 Effect of specimen length on stress-strain relationship under the same strain rate for (a) high-polymer-content sealant, and (b) crumb-rubber sealant

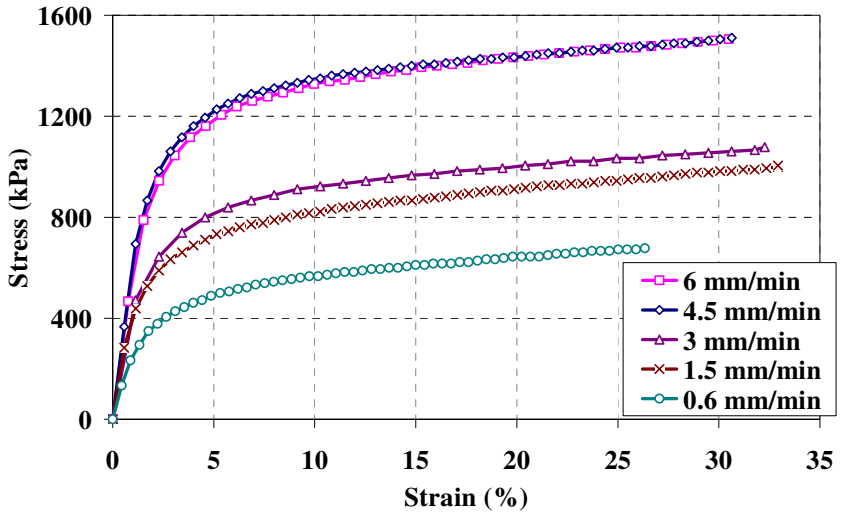
Figure 27 illustrates that specimen C elongates about two to three times specimen B. In addition, high-polymer-content sealants have shown 10 to 20 times more elongation and up to two times greater tensile strength than crumb-rubber sealants. Regardless of specimen geometry, high-polymer-content sealants have shown equivalent peak stress at its maximum elongation state. Hence, the length effect is negligible in the sealant tensile strength when high-polymer-content products are used.

Loading Rate Effect on Stress-Strain Response

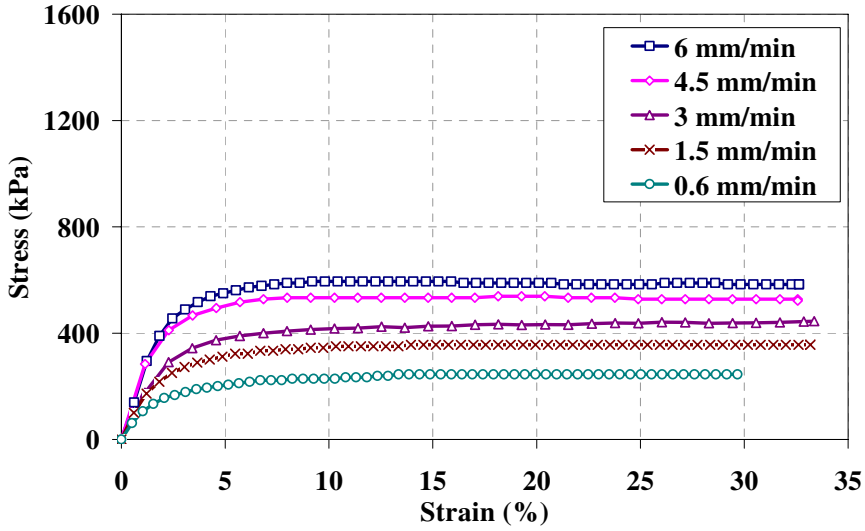
Figure 28 and 31 depict the stress-strain relationships for the type B specimen at various elongation rates. It is clear that the stress level increases with the increase in strain rate. As viscoelastic materials, sealants tend to relax the imposed stress over time; but at different levels. For example, sealant PP exhibits a cold drawing behavior as the stress becomes constant with increasing strain. This could be due to the chain-like molecules such as SBS in the sealant being drawn out of their original amorphous structure into an approximately linear and parallel arrangement. On the other hand, no clear cold drawing was observed for sealant WW at various strain rates.

The high-polymer-content sealant in general has shown ductile responses with no sign for failure up to 30% elongation. On the other hand, failures of the crumb rubber-modified sealant (YY and ZZ) occur at a strain level lower than 3%. Visual inspection has yielded that YY and ZZ specimens failed at the binder-rubber particle interface.

To identify an optimal elongation rate for testing sealants, a rate compatible with in-the-field crack movement at a low service temperature was considered. Generally, the crack opening rate in the field is extremely slow; the rate used in the current test is relatively high, which may increase the chance of debonding failure at the specimen-end tab interface. Based on laboratory testing, it was found that testing at an elongation rate between 1.5 to 3mm/min is appropriate.



(a) WW

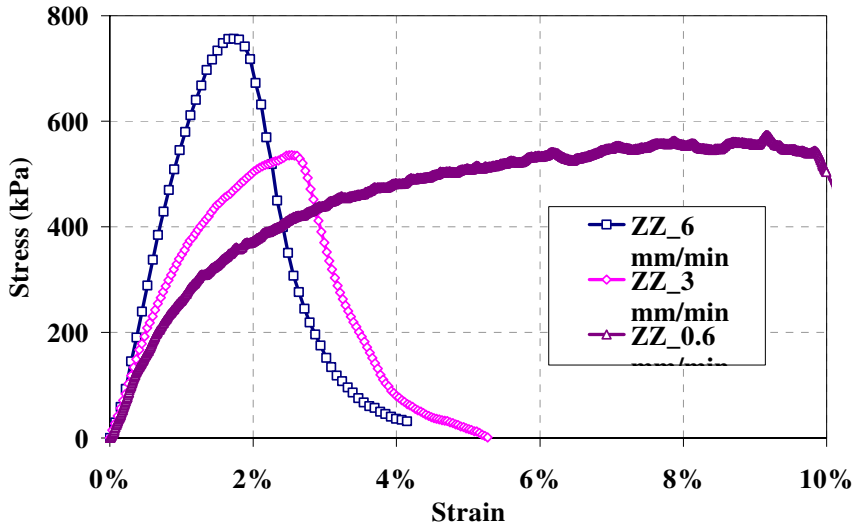


(b) PP

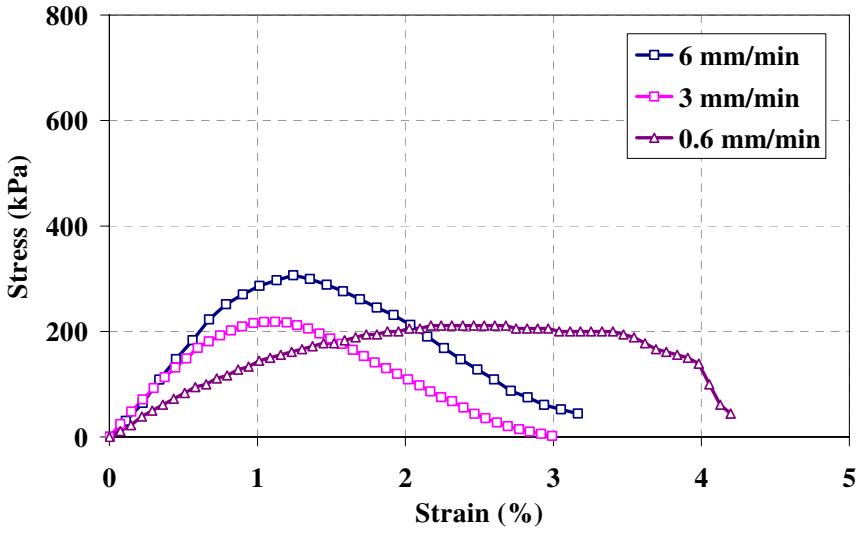
Figure 28 Stress-strain relationships at various elongation rates for high-polymer-content sealants (a) WW and (b) PP at -34°C

Temperature Effect on Percent Modulus Reduction

The second parameter investigated in this research is percent modulus reduction (M_r). Figure 30 to Figure 31 show the normalized relaxation moduli versus time at various temperatures for five sealants. Typically, the rate of moduli reduction increased with temperature increase. For instance, for sealant DD, the percent moduli reduction at -22°C was greater than the percentage at -34°C at a given time t (t=10s). This rate increase is also evident for sealant MM between -40°C and -34°C, sealant EE between -16°C and -10°C. However, for sealant UU, the difference was insignificant.



(a) ZZ



(b) YY

Figure 29 Stress-strain relationships at various elongation rates for crumb rubber-modified sealants (a) ZZ and (b) YY at -10°C

For sealant MM at -40°C, the data shows that elastic energy is still stored in the sealant throughout the loading process. This energy dissipates slowly, and if the specimen does not rupture, it will asymptotically approach a final non-zero plateau. On the other hand, at -34°C, the dissipation of stored energy for sealant MM is more rapid and greater mechanical relaxation occurs over a shorter time interval. This transition was not observed over the testing temperature for sealant UU. This implies that sealant UU is less sensitive to temperature at that temperature range.

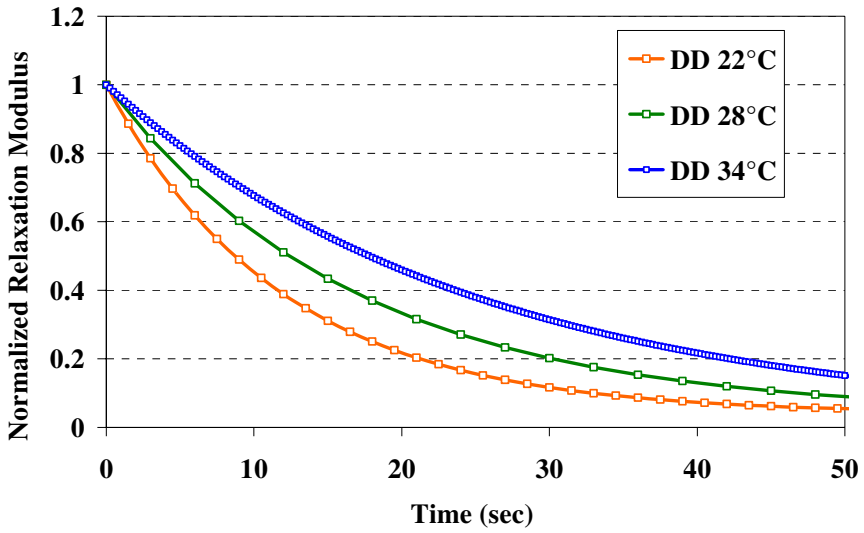


Figure 30 Stress relaxation behavior of sealant DD at various isothermal temperatures

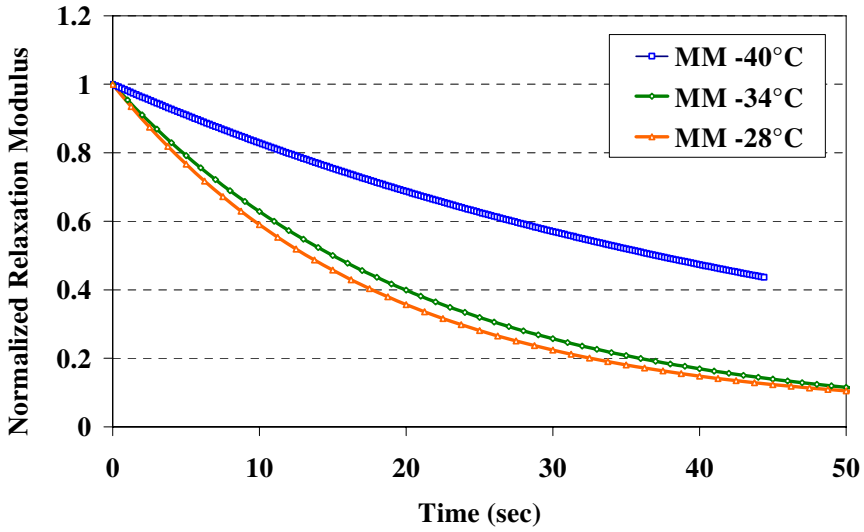


Figure 31 Stress relaxation behavior of sealant MM at various isothermal temperatures

TEST VARIATIONS

Precision and bias are two of the most important factors that must be considered while developing performance-based guidelines. Single operator precision (repeatability) results as defined in ASTM C670, is presented in Figures 37 through 39 for extendibility, maximum stress, and SED. Precision measures the greatest difference between two or more test results that would be considered acceptable when a test is conducted properly. For all sealants, the repeatability as conducted by a single operator is less than 10% and this suggests that the test is repeatable.

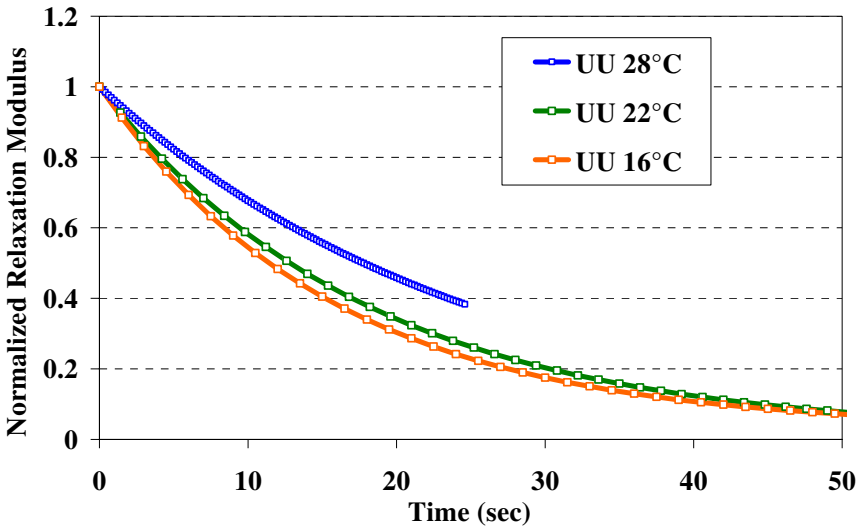


Figure 32 Stress relaxation behavior of sealant UU at various isothermal temperatures.

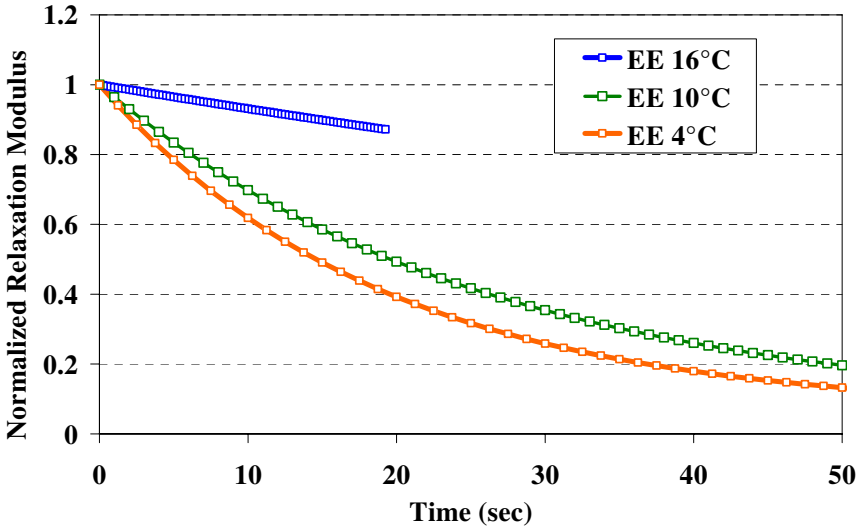


Figure 33 Stress relaxation behavior of sealant EE at various isothermal temperatures.

Aged Sealants BB, MM, AE, and ZZ were selected to conduct operator variation testing. A statistical t-test, assuming that two samples have equal variance, was conducted to determine significant differences among operators. No significant differences were detected for the extendibility measured by the two operators at the 95% confidence level.

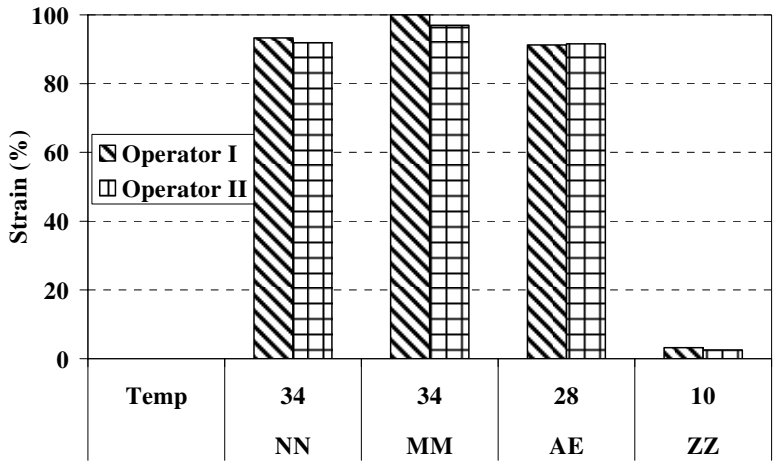


Figure 34 Comparison of test results for average failure strain of selected sealants from two operators

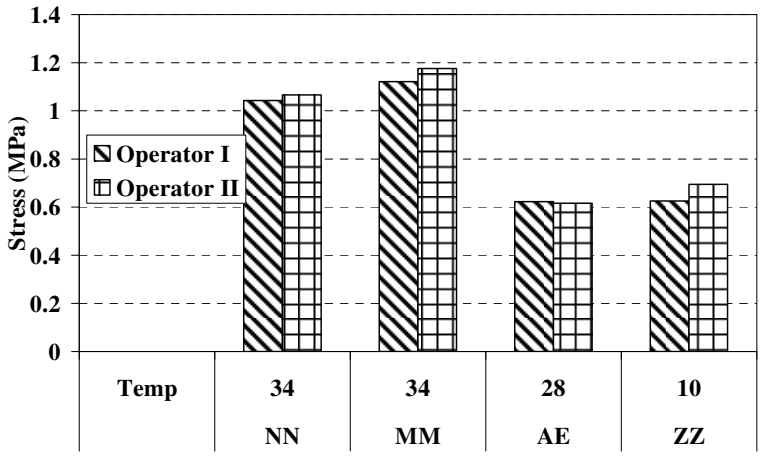


Figure 35 Comparison of test results for average failure stress of selected sealants from two operators

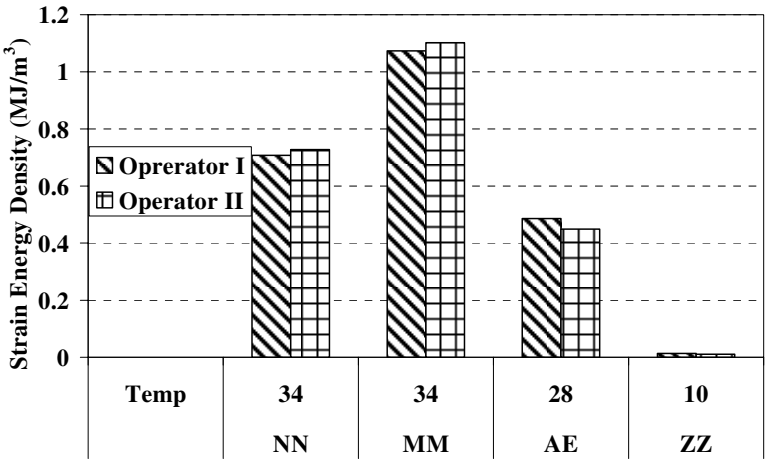


Figure 36 Comparison of test results for average strain energy density of selected sealants from two operators

CONCLUSIONS

A modified direct tension test (DTT), crack sealant direct tension test (CSDTT), was found to be suitable for evaluating crack sealant behavior at low temperature. The following parameters were considered in the development of the test: simulation of sealant loading condition when a crack moves, ease of measurement and calculation, and test repeatability. An optimized testing specimen size was developed and a modified testing procedure was introduced for crack sealant. The CSDTT specimen, a shorter and thinner version of the standard DT specimen, was found to be easy to prepare and better simulate sealant field elongation. The new specimen geometry allows sealant to be stretched up to 95% strain, which meets the extreme service conditions that sealants experience in the field. Fifteen sealants were tested at low temperatures ranging from -40 to -4°C. Three performance parameters were identified to evaluate the crack sealants' performance at low temperature: extendibility, modulus reduction percentage after 10s of loading, and strain energy density. The relaxation modulus reduction percentage gives an indication of a material's ability to relax the imposed loading. It is desirable to have a high SED; but it has to be accompanied with high extendibility. The extendibility is a good criterion for identifying and distinguishing among sealants. For simplicity, extendibility parameter is recommended for measurement as part of the performance-based guidelines for the selection of hot-poured crack sealants.

RECOMMENDATION

The study recommends using the CSDTT as a standard test to evaluate the bituminous-based hot-poured crack sealant at low temperature. Extendibility is selected as a performance parameters and is recommended for use in performance-based guidelines for the selection of hot-poured crack sealants. The threshold for the extendibility dependents on sealants' lowest application temperature and is presented in the Table 11. In addition, because the test is conducted under a relatively higher deformation rate compared to field crack movement, it is recommended that a +6°C shift be used for sealant testing to simulate low field temperature. For example, if the lowest application temperature is determined -16°C, the test should be conducted at -10°C. If the extendibility of the sealant at -10°C is over 25%, the sealant passes

the criterion and will be approved for use. The recommended thresholds for the extensibility at various temperatures follow (Table 11):

Table 11 Threshold for extendibility at various temperatures

Temperature (°C)	-4	-10	-16	-22	-28	-34	-40
Extendibility (%)	10	25	40	55	70	85	85

REFERENCES

ABAQUS. Finite Element Computer Program. *Theory Manual*. Version 6.5-1, Hibbit, Karlsson and Sorensen, Inc., Pawtucket, RI, 2005.

Al-Qadi, I. L., Masson, J-F, Loulizi, A., Collins, P., McGhee, K., Woods, J., and Bundalo-Perc, S. Long-Term Aging and Low Temperature Testing. Report B5508.5, National Research Council, Ottawa, Canada, 2003.

Al-Qadi, I.L, S.H. Yang, S. Dessouky, J.F. Masson, A. Loulizi, and M. Elseifi, "Development of Crack Sealant Bending Beam Rheometer (CSBBR) Testing to Characterize Hot-Poured Bituminous Crack Sealant at Low Temperature," In *The Journal of AAPT*, Vol. 76, 2007, pp. 85-122.

Al-Qadi, I. L, Yang, S. H., Dessouky, S., Masson, J.-F. Low Temperature Characterization of Hot-Poured Crack Sealant Using Modified SHRP Direct Tensile Tester. In *Journal of the Transportation Research Record*, No. 1991, Transportation Research Board, National Academies, Washington, DC, Oct 2007, pp. 109-118.

Anderson, D. A., Christensen, D. W., Bahia, H. U., Dongre, R., Sharma, M. G., Antle, C. E., and Button, J. *Binder Characterization and Evaluation. Volume 3: Physical Characterization*. SHRP-A-369 Final Report, Strategic Highway Research Program, National Research Council, Washington, DC, 1994.

Basu, A., Marasteanu, M. O., and Hesp, S. A. M. Time-Temperature Superposition and Physical Hardening Effects in Low-Temperature Asphalt Binder Grading. Paper Presented at the 82nd Annual Meeting of the Transportation Research Board, Washington, DC, 2003.

Belangie, M. C., and Anderson, D. I. Crack Sealing Methods and Materials for Flexible Pavements. Final Report No. FHWA-UT-85-1, Utah Department of Transportation, Salt Lake City, UT, 1985.

Berry, J. P. Strength of Glass Polymer. *Journal of Polymer Science*, Vol. 50, 1961, pp107.

Bouldin, M. G., Dongré, R., Sharrock, M. J., Rowe, G.M., Anderson, D.A., Marasteanu, M., Dunn., L., Zanzotto, L., and Kluttz, R.Q. A Cmprehensive Evaluation of the Binders and Mixtures Placed on the Lamont Test Sections. Report prepared for the FHWA Binder ETG, Federal Highway Administration, Washington, D.C., 1999.

Chehovits, J., and Manning, M. Materials and Methods for Sealing Cracks in Asphalt Concrete Pavements. In Transportation *Research Record 990.* Transportation Research Record, National Research Council, Washington DC, 1984, pp. 21-30.

Chong, G. J. Rout and Seal Cracks in Flexible Pavements—A Cost-Effective Preventive Maintenance Procedure. In *Transportation Research Record 1268*. Transportation Research Record, National Research Council, Washington DC, 1990, pp. 8-16.

Chong, G. J. and Phang, W. A. *Improved Preventive Maintenance: Sealing Cracks in Flexible Pavements in Cold Regions.* Report PAV-87-01. Ontario Ministry of Transportation, Downsview, ON, 1987.

Cominsky, R. J., Huber, G. A., Kennedy, T. W., and Anderson, M. *The Superpave Mix Design Manual for New Construction and Overlays*. SHRP-A-407 Final Report. Strategic Highway Research Program, National Research Council, Washington, DC, 1994.

Cook, J. P., Weisgerber, F. E., and Minkarah, I. A. *Evaluation of Joint and Crack Sealants*. FHWA/OH-91/007, University of Cincinnati, Cincinnati, OH, 1990.

Cuelho, E., Ganeshan, S. K., Johnson, D. R., Freeman, R. B., and Schillings, P. L. Relative Performance of Crack Sealing Materials and Techniques for Asphalt Pavements. *Third International Symposium on Maintenance and Rehabilitation of Pavements and Technological Control*, July 7–10, Guimarães, Portugal, 2003, pp. 327–337.

Cuelho, E., Johnson, D. R., and Freeman, R. B. *Cost-Effectiveness of Crack Sealing Materials and Techniques for Asphalt Pavements*. FHWA/MT-02-002/8127. Montana Department of Transportation, Helena, MT, 2002, 247 pp.

Dessouky, S., and Al-Qadi, I. L. Linear Viscoelastic Constitutive Model for Hot-Poured Crack Sealants at Low Temperatures and Strain Levels Using a Prony Series. Submitted to ASCE for review, 2006.

Dongre, R., Button, J. W., Kluttz, R. Q., and Anderson, D. A. Evaluation of Superpave Binder Specification with Performance of Polymer-Modified Asphalt Pavements. *ASTM Special Technical Publication, Vol. 1322*, Sep. 1997, pp. 80-100.

Dowling, N. E. *Mechanical Behavior of Materials* (Second Edition), Prentice Hall, Upper Saddle River, NJ, 1999.

Eaton, R. A., and Ashcraft, J. *State-of-the-Art Survey of Flexible Pavement Crack Sealing Procedures in the United States*. Report 92-18. Cold Regions Research & Engineering Laboratory, U.S. Army Corps of Engineers, Hanover, NH, 1992.

Elseifi, M., Dessouky, S., Al-Qadi, I. L., and Yang, S. H. A Viscoelastic Model to Describe the Mechanical Response of Bituminous Sealants at Low Temperature. Presented at the 85th Annual Meeting of the Transportation Research Board, Washington, DC, 2006.

Fang, C., Galal, K. A., Ward, D. R., Haddock, J. E., and Kuczek, T. Cost-Effectiveness of Joint and Crack Sealing. Presented at the 82nd Annual Meeting of the Transportation Research Board, Washington, DC, 2003.

Ferry, J. D. *Viscoelastic Properties of Polymers*. 3rd Ed, Wiley, New York, 1980.

Findley, W. N., Lai, J. S., and Onaran, K. C*reep and Relaxation of Nonlinear Viscoelastic Materials*. North Holland, Amsterdam, 1976.

Georgia DOT Standard Specification for Asphalt-Rubber Joint and Crack Seal, National Highway Specification. Available from http://fhwapap04.fhwa.dot.gov/nhswp.html [Access 5 January 2007].

Griffith, A. A. The Phenomena of Rupture and Flow in Solids. *Phil. Trans. Royal. Society London*, A, V. 221, 1921, pp.163-198.

Hills, J. F. and Brien, D. The Fracture of Bitumens and Asphalt Mixes by Temperature Induced Stresses. Proceedings of the *Journal of Association of Asphalt Paving Technologists,* Vol. 35, 1996, pp. 292–309.

Ho, S. M. S., and Zanzotto, L. Sample Preparation for Direct Tension Testing – Improving Determination of Asphalt Binder Failure Stress and Test Repeatability. In *Transportation Research Record 1766*. Transportation Research Board, Washington, DC, 2000, pp. 15-23.

Johansson, L. S. and Isacsson, U. Effect of Filler on Low Temperature Physical Hardening of Bitumen. *Construction and Building Materials*, Vol. 12, 1998, pp. 463-470.

Joseph, P. *Field Evaluation of Rout and Seal Crack Treatment in Flexible Pavement*. Report PAV-90-03, Ministry of Transportation of Ontario, Downsview, ON, 1990.

Ketcham, S. *Sealants and Cold Regions Pavement Seals*. CRREL Report 95-11, U.S. Army Corps of Engineers, 1995.

Khuri, M. F., and Tons, E. Comparing Rectangular and Trapezoidal Seals Using the Finite Element Method. In *Transportation Research Record 1334*. Transportation Research Board, Washington, DC, 1993, pp. 25-37.

Kim, Y. R. and Little, D. N. Linear Viscoelastic Analysis of Asphalt Mastics. *Journal of Materials in Civil Engineering*, ASCE, Vol. 16, No. 2, 2004, pp. 122-132.

Linde, S. Investigations on the Cracking Behavior of Joints in Airfields and Roads: Field Investigations and Laboratory Simulation. SP Report 1988:23. Swedish National Testing Institute, Borås, Sweden, 1988.

Marasteanu, M. O., and Anderson, D. A. Comparison of Moduli for Asphalt Binder Obtained from Different Test Device. *Journal of the Association of Asphalt Paving Technologists*, Vol.68, 2000, pp. 574-607.

Masson, J.-F. Bituminous Sealants for Pavement Joints and Cracks: Building the Basis for a Performance-Based Specification. In *Durability of Building and Construction Sealants*. A. Wolf, Ed., RILEM, Paris, 2000, pp. 315-328.

Masson, J-F and Al-Qadi, I. L. Long-Term Accelerated Aging and Low Temperature BBR Testing of Sealants. National Research Council of Canada, Report No. B5508.5, 2004.

Masson, J.-F., Collins, P., and Légaré, P. P. Performance of Pavement Crack Sealants in Cold Urban Conditions. Canadian *Journal of Civil Engineering*. Vol. 26, No. 4, 1999, pp. 395-401.

Masson, J-F., Collins, P., Margeson, J., and Polomark, G. Analysis of Bituminous Crack Sealants by Physicochemical Methods: Relationship to Field Performance. In

Transportation Research Record 1795, Transportation Research Board, Washington, DC, 2002, pp. 33-39.

Masson, J-F., Collins, P., Wood, J. R., and Bundalo-Perc, S. Degradation of Bituminous Sealants Due to Extended Heating before Installation, 85th Transportation Research Board Annual Meeting, Washington, D.C., 2006.

Masson, J.-F., and Lacasse, M. A. Considerations for a Performance-Based Specification for Bituminous Crack Sealants. In *Flexible Pavement Rehabilitation and Maintenance, ASTM Special Publication STP1348*. American Society for Testing and Materials, 1998.

Masson, J.-F., and Lacasse, M. A. Effect of Hot-Air Lance on Crack Sealant Adhesion. *Journal of Transportation Engineering*, ASCE, Vol. 125, No. 4, 1999, pp. 357-363.

Masson, J.-F., Woods, P., Collins, P., and Al-Qadi, I. L. Accelerated Aging of Bituminous Sealants: Small Kettle Aging. Paper submitted to the 86th Annual Meeting of the Transportation Research Board, Washington, DC, 2007.

Park, S.W., and Kim, Y. R. Fitting Prony-Series Viscoelastic Models with Power-Law Presmoothing. *Journal of Materials in Civil Engineering*, ASCE, Vol. 13, No. 1, 2001, pp. 26-32.

Park, S. W., and Schapery, R. A. Methods of Interconversion between Linear Viscoelastic Material Functions. Part I—A Numerical Method Based on Prony series. *International Journal of Solids and Structures*, Vol. 36, 1990, pp. 1653-1675.

Petersen, J. C., Robertson, R. E., Branthaver, J. F., Harnsberger, P. M., Duval J. J., Kim, S. S., Anderson, D. A., Christiansen, D. W., Bahia, H. U., Dongre, R., Antle, C. E., Sharma, M. G., Button, J. W., and Glover, C. J. *Binder Evaluation and Characterization – Volume 4: Test Methods*. SHRP-A-370 Final Report, Strategic Highway Research Program, National Research Council, Washington, DC, 1994.

Rivlin, R. S. and Thomas, A. G. Rupture of Rubber. I. Characteristic Energy for Tearing. *Journal of Polymer. Science*, Vol. 10, 1953, pp.291-318.

Rosen, B., ed. *Fracture Processes in Polymeric Solids*. Interscience, New York, 1964.

Schapery, R. A., and Park, S. W. Methods of Interconversion between Linear Viscoelastic Material Functions, Part II—An Approximate Analytical Method. *International Journal of Solids and Structures*, Vol. 36, No.11, 1999, pp. 1677-1699.

Smith, Y. L. Linear Viscoelastic Response to a Deformation at Constant Rate: Derivation of Physical Properties of a Densely Crosslinked Elastomer. *Transactions of the Society of Rheology*, Vol 20, No 2, 1976, pp. 103-117.

Smith, K. L., and Romine, A. R. *Innovative Materials Development and Testing Volume 3: Treatment of Cracks in Asphalt Concrete-Surfaced Pavements*. SHRP-H-354. Strategic Highway Research Program, National Research Council, Washington, DC, 1993.

Smith, K. L., and Romine, A. R. *LTPP Pavement Maintenance Materials: SHRP Crack Treatment Experiment*. FHWA-RD-99-143, Final Report. FHWA, Washingtion, DC, 1999, 163 pp.

Tay, A. O. and Teoh, S. H. A Numerical Method for Determining Tensile Stress-Strain Properties of Plastics from Total Elongation Measurements, *Polymer Testing*, Vol 8, I. 4, 1989, pp. 231-248.

Treloar, L. R. G. The Elasticity and Related Properties of Rubbers. *Rubber Chemistry and Technology*, Vol. 47, 1974, pp. 625–696.

Yang, S. H., and Al-Qadi, I. L. A Modified Direct Tension Test (DTT) for Bituminous Crack Sealant Characterization at Low Temperature," Proceedings of *Journal of the Association of Asphalt Paving Technologists*, 2008 (Accepted).

Ward, D. R. Evaluation of the Implementation of Hot-Pour Sealants and Equipment for Crack Sealing in Indiana. FHWA/IN/JTRP-2000/27, FHWA, Washington, DC, 2001, 189 pp.

Yang, S. H., and I. L. Al-Qadi, "A Modified Direct Tension Test (DTT) for Bituminous Crack Sealant Characterization at Low Temperature," In *the Journal of the AAPT* , Vol 77, 2008.

Zanzotto, L. *Laboratory Testing of Crack Sealing Materials for Flexible Pavements*. Final Report. Transportation Association of Canada, Ottawa, Ontario, 1996.

Zhai, H. and Salomon, D. Evaluation of Low Temperatures of Asphalt Crack Sealants Using the Direct Tension Tester. Proceedings of the 50th Canadian Technical Asphalt Association, Victoria, Canada, 2005.

Zhang, X., and Huber, G. Effect of Asphalt Binder on Pavement Performance: An Investigation Using the SuperPave Mix Design System. Proceedings of *Journal of the Association of Asphalt Paving Technologists*, Vol. 65, 1996, pp. 449-490.

APPENDIX A

CSDTT Testing Procedure



Step 1: Take test sample (in this case, Sealant L) from freezer and place on lab table about 12–24 hrs before testing. This allows for test sample to adjust to ambient temperature (room temperature).



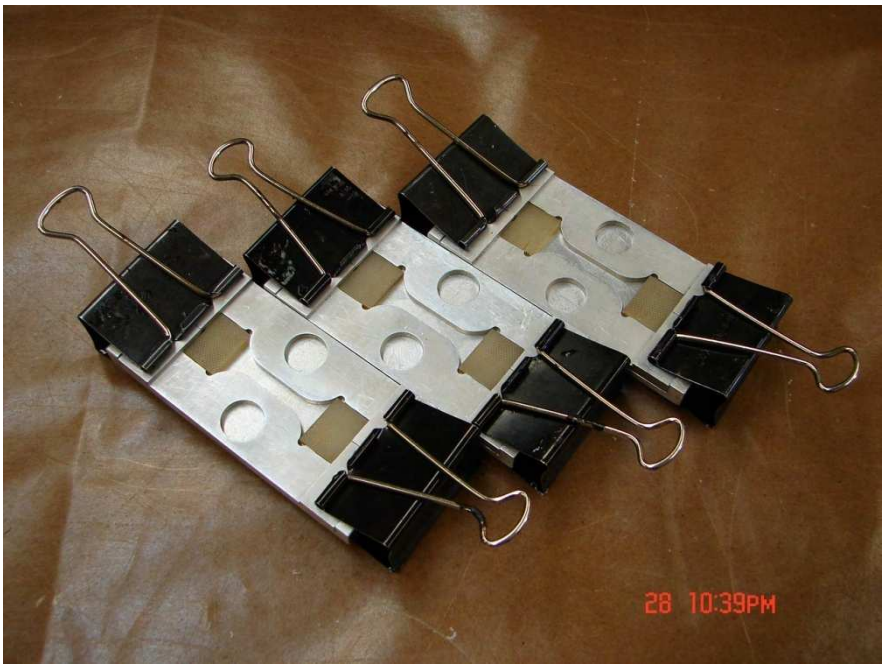
Step 2: Heat a conventional laboratory oven A to the recommended pouring temperature (T°C).



Step 3: Heat a conventional laboratory oven B to 50°C blow below the recommended pouring temperature.



Step 4: Spray release agent (Nix Stix X-9032 from Dwight Products) onto test sample mold.



Step 5: Place the end tabs into the mold and use 50-mm binder clips to hold the various mold pieces in place.



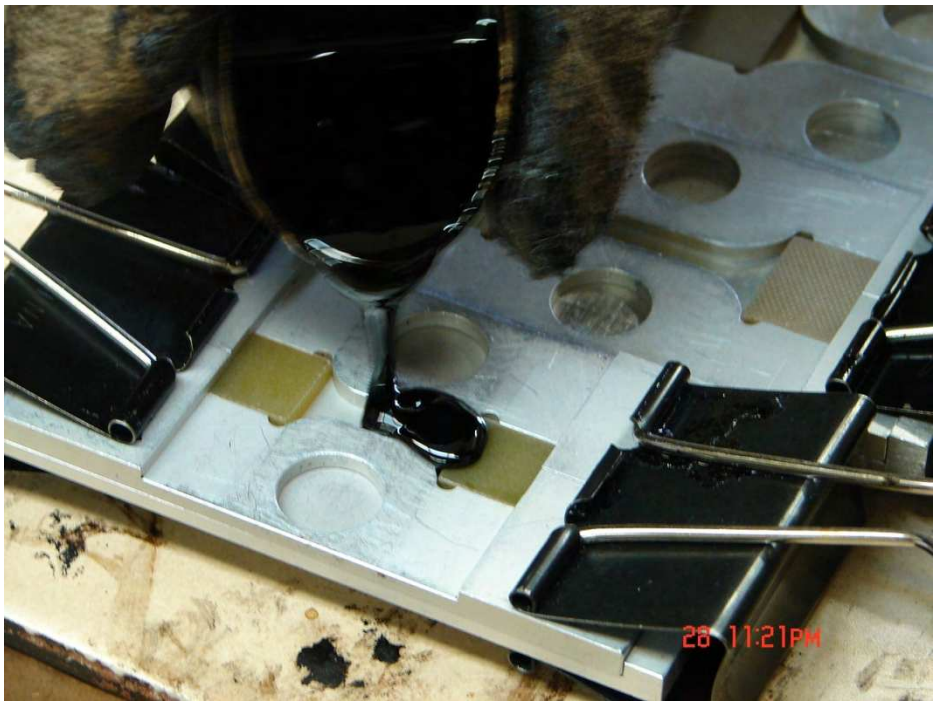
Step 6: Place test samples into oven A when oven temperature reaches T°C. Be sure to log the time when test samples are placed into the oven.



Step 7: After sealant is placed in oven B for 15min, place empty molds on the preheated ceramic tile in oven B, which is preheated to 50°C lower than recommended pouring temperature (T-50°C) for 15mins.



Step 8: 15min after placing test samples into heated oven A, stir the samples to ensure that sediments in the sample are thoroughly mixed and distributed. Be sure to scrape the bottom and sides of the canister. Place the test samples back into the oven after stirring.



Step 9: After sample is heated in oven A for 30min, take out sealant and pour the material into the preheated molds, which are still on the preheated ceramic tile. This action prevents the sealant from cooling down too rapidly. Be sure to pour from one end of the mold and proceed slowly towards the opposite end.



Step 10: Use a heated spatula to gently apply pressure at the interface of sealant and end tabs. This will improve bonding between the sealant and the end tabs.



Step 11: Allow the test specimens to cool for 1hr at room temperature.



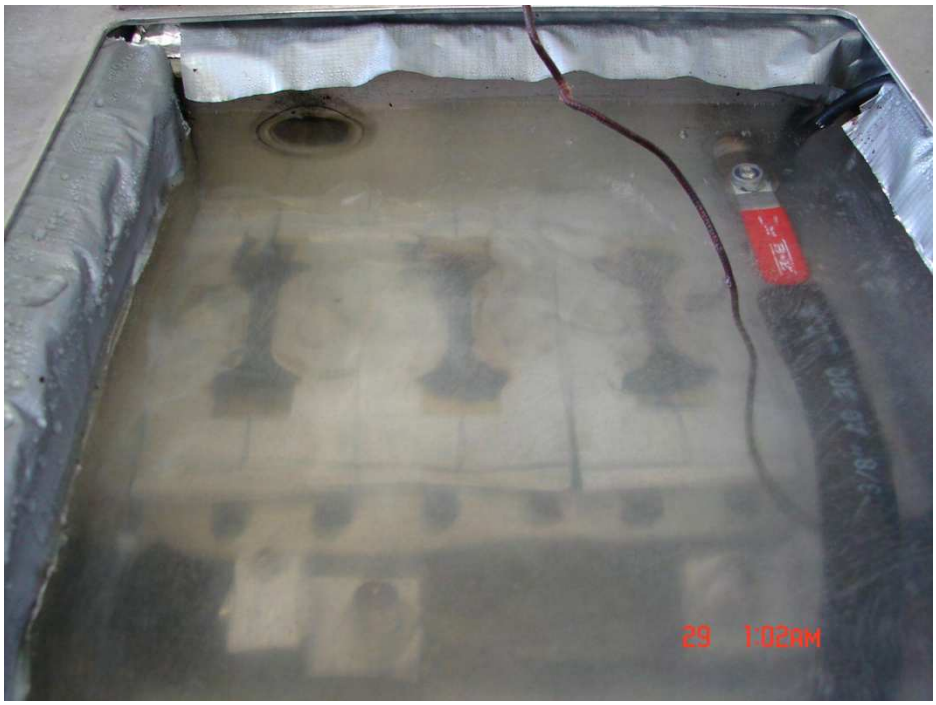
Step 12: Use a propane blow torch to heat a cutting knife.



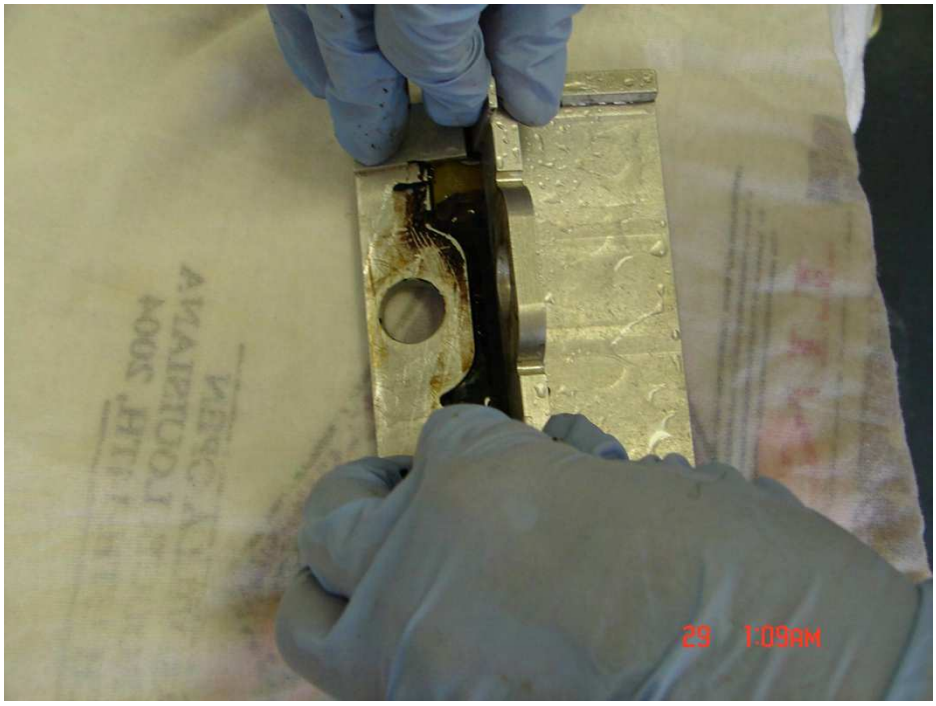
Step 13: Angle the mold downward and trim the excess sealants from the test mold.



Step 14: The specimens should be flush with the top of the molds without any visible deformation. Unclamp the mold.



Step 15: Once the molds have been unclamped, place them individually into an alcohol bath. Allow the samples to stay in the bath for 5min.



Step 16: Take out the mold and place it on a flat surface to demold the sealant.



Step 17: Place the demolded specimens in the bath for one hour, and then proceed with testing.

APPENDIX B

Determination of effective gauge length FOR test SPECIMENS

The method suggested by Tay and Teoh (1989) to determine the effective gauge length for test specimens is simply the following: It is stated that the elongation of a standard dog-bone-shaped test specimen due to an applied axial load P is equivalent to that of a simple rectangular specimen with the same cross-sectional dimensions of the restricted section and with an effective gauge length, L_{eff}. The total elongation of the standard specimen shown in Figure B-1 is given as follows:

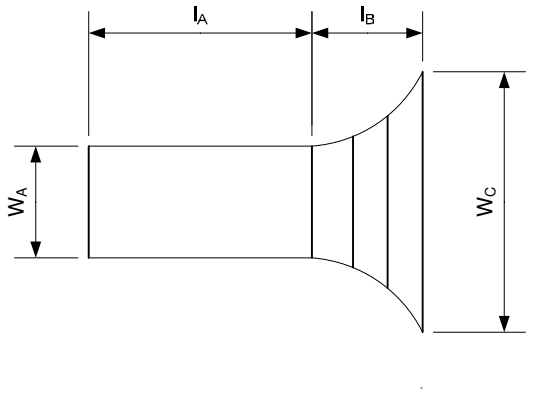


Figure B-1 Symmetrical half of dog-bone-shaped tensile test specimen.

$$\delta_T=2(\delta_A+\delta_B) \tag{B-1}$$

where δ_A and δ_B are the extensions of the restricted section 1_A (Figure B-1) and the transition section 1_B.

Hence,

$$\delta = \frac{PL_{eff}}{AE} \tag{B-2}$$

where A is the cross-sectional area of the restricted section and E is the modulus of elasticity. Therefore,

$$L_{eff} = \frac{2AE}{P}(\delta_A + \delta_B) = \frac{2E}{\sigma}(\delta_A + \delta_B) \tag{B-3}$$

The effective gauge length for any standard geometry can be calculated from Equation B-3. To obtain the stress in the restricted section of the specimen, a finite element analysis was conducted (Figure B-2). The stress in the middle portion of the specimen is 1.65MPa, with a Young's modulus of 33.5MPa and δ_T=1. With these values, the effective gauge length of 20.3mm can be obtained.

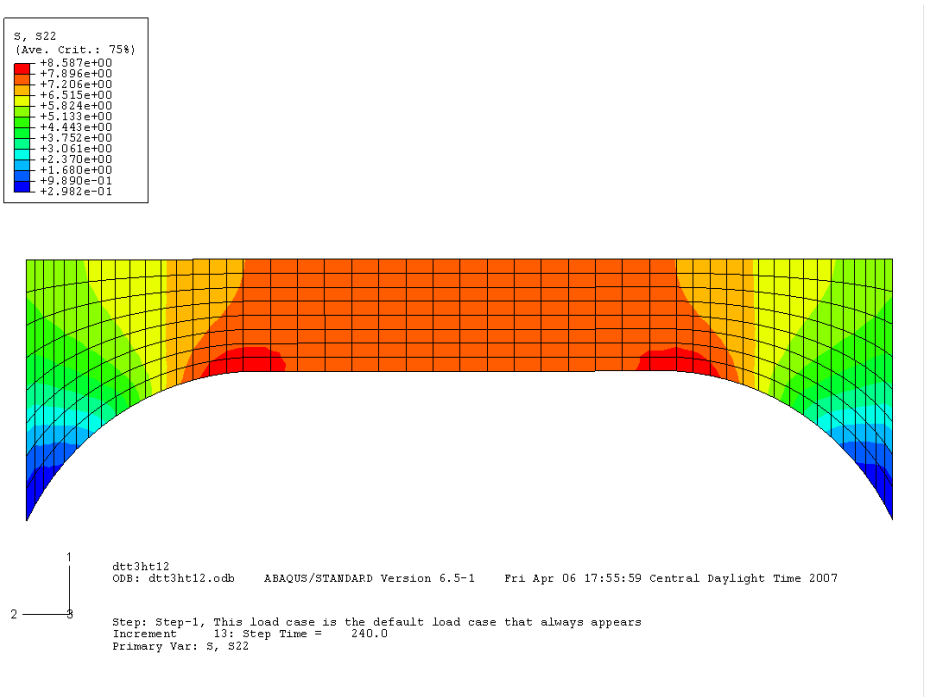


Figure B-2 Stress distribution in two directions in the restricted section of a specimen.

APPENDIX C

Specification

Evaluation of the Low Temperature Tensile Property of Bituminous Sealants by Direct Tension Test
Sealant Consortium Designation: SC-6

1. SCOPE

1.1. This method applies to bituminous sealants used in the construction and maintenance of roadways.

1.2. The method is used to determine the extensibility and strain energy density (SED) of sealants at low temperature. It can be used with unaged material or with material aged using Test Method SC-3 (Vacuum Oven Aging). The test apparatus is designed for testing within the temperature range from -4°C to -40°C.

1.3. This practice covers the determination of extensibility and percent modulus decay in bituminous sealants with the use of direct tension testing and by applying tensile stress-strain test.

2. REFERENCED DOCUMENTS

2.1. AASHTO Standards:

T314, Determining the Fracture Properties of Asphalt Binder in Direct Tension (DT).

2.2. ASTM Standards:

D6723, Standard Test Method for Determining the Fracture Properties of Asphalt Binder in Direct Tension (DT).

D5167, Standard Practice for Melting Hot-Applied Joint and Crack Sealant and Filler for Evaluation.

D6373, Standard Specification for Performance Graded Asphalt Binder.

E77, Test Method for the Inspection and Verification of Thermometers

E145, Standard Specification for Gravity-Convection and Forced-Ventilation Ovens.

2.3. N. E. Dowling. Mechanical Behavior of Materials (Second Edition). Prentice Hall, Upper Saddle River, NJ, 1999.

2.4. Documents of the Sealant Consortium (SC):

SC-1, Guidelines for Graded Bituminous Sealants

SC-2, Test Method for Measuring Apparent Viscosity of Hot-poured Crack Sealant using Brookfield Rotational Viscometer RV.

SC-3, Method for the Accelerated Aging of Bituminous Sealants.

SC-4, Method to Evaluation of the Tracking Resistance of Bituminous Sealants and Fillers by Dynamic Shear Rheometry.

SC-5, Method to Measure Low Temperature Sealant Flexural Creep Stiffness at Low Temperature by Bending Beam Rheometer.

SC-6, Method to Evaluate Sealant Extensibility at Low Temperature by Direct Tension Test.

SC-7, Blister Method to Predict the Adhesion of Bituminous Sealants.

3. TERMINOLOGY

3.1. Bituminous sealants are hot-poured modified asphaltic materials used in pavement cracks and joints.

3.2. Effective gauge length. Elongation of a standard dog bone shaped test specimen due to an applied axial load P is equivalent to that of a simple rectangular specimen with the same cross-sectional dimensions of the restricted section. Effective gauge length, L_{eff}, is defined as the length of the simple rectangular specimen and has been determined to be 20.3mm.

3.3. Tensile stress. Tensile load divided by the true area of cross-section of the specimen.

3.4. Tensile strain. Change in the effective gauge length by the application of tensile load divided by the original unloaded effective gauge length.

3.5. Brittle material. The stress-strain curve is linear up to fracture at about 1% to 2% elongation.

3.6. Brittle-ductile material. The stress-strain curve is curvelinear and the stress is gradually reduced after the peak point. The failure happens by gradually breaking the molecular bond within the material.

3.7. Ductile material. The material does not rupture in the direct tension test but elongates due to high strain.

3.8. Rubbery behavior. Materials that exhibit rubbery behavior can be stretched to extreme elongation without rupture.

3.9. Percent modulus decay. The percentage modulus deduction after 10sec of loading.

4. SUMMARY OF PRACTICE

4.1. This practice contains the procedure to measure the extensibility and the strain energy density of a bituminous sealant or filler using direct tension test (DTT). The material is bonded between two end-tabs made by Plexiglass and subjected to a constant strain rate at a specific temperature.

4.2. The test method is developed to select the bituminous sealant at temperatures where they exhibit rubbery behavior.

4.3. A linear variable differential transformer (LVDT) is used to measure the elongation of the test specimen as it is pulled in tension at a constant strain rate of 6%/min

(1.2mm/min). A load cell is used to monitor the load during the test. The stress and strain at the point of rupture or peak load are reported.

5. SIGNIFICANCE AND USE

5.1. This test is intended for bituminous sealants applied to roadway joints and cracks.

5.2. The test temperature is determined to be the lowest temperature experienced by the pavement surface in the geographical area for which the sealant is intended.

5.3. The sealant extensibility is a parameter of the capacity of sealant to sustain large deformations due to crack expansion at low temperature without fracture.

5.4. The percent modulus decay is an indication of how fast the sealant can release the imposed loading. A higher percentage decay represents that the sealant can relax the load faster.

5.5. This method is intended for aged sealants, which could become stiffer or softer with age.

6. APPARATUS

6.1. Direct Tension Test (DTT) Device – The DTT system consists of two metal grips to hold the specimen, an environment chamber, a loading device, and a control and data acquisition system. The instrument must meet the requirements stated in AASHTO T314.

6.2. Specimen End Tabs and Gripping System – End tabs made from Plexiglass material having dimensions as described in Figure 1 that shall be bonded to both ends of the test specimen to transfer the tensile load to the sealant. The manufacturing requirement of the end tabs and the gripping system shall meet the requirement in AASHTO T314.

6.3. Chiller and test chamber – A calibrated circulated temperature control system shall have temperature range from -4°C to -40°C. The insulated test chamber shall be capable of maintaining a temperature of ± 0.1°C.

6.4. Specimen molds – The specimen molds should be made from aluminum. Molds shall have dimension as specified in Figure 1. A silicon-based release agent as described later in 7.2 shall be used to prevent sealant from adhering to the aluminum molds.

6.5. Laboratory Ovens – two standard laboratory ovens – Two forced-air convection ovens capable of producingreaching and maintaining a temperature of 200 ± 0.± 5°C. for heating sealant and molds.

7. REAGENTS AND MATERIALS

7.1. Fluid for Test Chamber – A fluid that is not absorbed by or does not affect the properties of the crack sealant being tested. The bath fluid shall be optically clear at the test temperature. Ethyl alcohol is suggested to use as a fluid for temperature control. The aqueous mixture of potassium acetate and deionized water used in the AASHTO T314 has been found to form turbid solution at temperature of -40°C.

7.2. Release Agent – A proper release agent to prevent crack sealant sticking to the mold. A silicon-based released agent is recommended.

7.3. Solvent – A solvent can properly clean the molds, end tabs, and plates. The parts cleaned by the solvent shall be submerged in the ethyl alcohol prior to use. This ensures the proper bond between sealant and end tabs.

7.4. Cleaning Cloths – Cloths for wiping molds, end tabs, and plates.

8. HAZARDS

8.1. Standard laboratory caution should be used in handling hot sealant in accordance to ASTM D5167, and required safety procedures should be followed when chemical agents are used.

9. VERIFICATION AND CALIBRATION

9.1. DTT – Follow the procedure as stated in AASHTO T314.

9.2. Oven and freezer – Calibrate the temperature with a thermometer that meets the requirements of ASTM E1. The thermometer calibration can be verified according to ASTM E77.

10. SAMPLES PREPARATION

10.1. Sample and prepare sealant according to ASTM D5167. See Note 1.

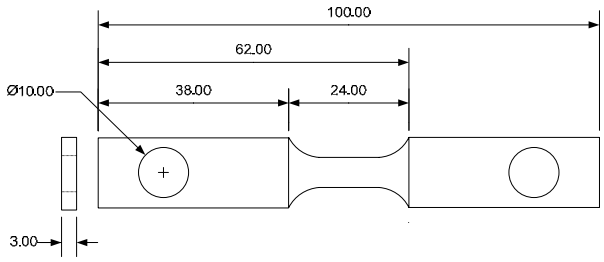
Note 1 – It is advantageous to sample about 500g sealant and sequentially pour specimens for all the tests, including the aging test (SC-3), the low temperature tests (SC-4 and SC-5), and the adhesion test (SC-6).

10.2. Anneal the sealant from which the test specimen is obtained by heating for 30 minutes. After 15 minutes, place the sealant in the oven, remove the sealant from the oven shortly, and stir the sealant by spatula to prevent segregation.

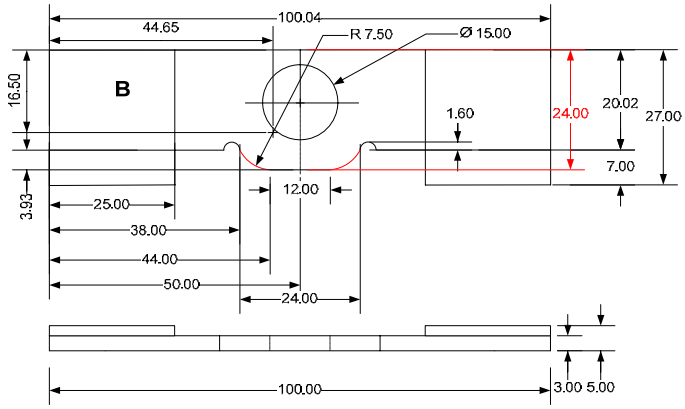
10.3. Follow the procedure 9.2 to 9.6 in AASHTO T314 with the following modification. See note 2 and 3.

Note 2 – If spray-type silicon based release agent is used, start from one side of the mold and slowly move toward the other side. Only one spray should be applied to the mold.

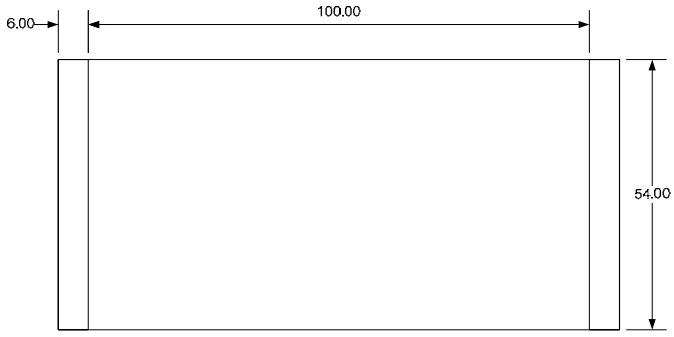
Note 3 – Place the molds and end tab assembly on top of a ceramic tile heated to 50°C lower than sealant pouring temperature. The ceramic tile should be placed in the preheated oven for 15 minutes.



End Insert



Mold Half



Mold Base

Figure 1. Dimension for DTT, end insert, and mold

11. CONDITIONING

11.1. Follow the procedure as stated in AASHTO T314.

12. PROCEDURE

12.1. Bring the DTT chamber to the test temperature (see Note 4).

Note 4: Select test temperatures in accordance with the material specification, e.g., SC-1, ASTM D6373-99.

12.2. Prepare four test specimens according to section 10.

12.3. Follow the procedure 12.2 to 12.3 in AASHTO T314 with the modification as in notes 5 and 6.

Note 5 – Adjust the load frame to allow 20mm traveling distance then place the specimen on the loading pin. Remove the slack between the specimen and the loading pins.

Note 6 – Manually adjust the stroke from the control screen/ panel to apply tension in the specimen until a load of 1±0.5 N is shown on the screen. Then calibrate the stroke and load back to zero.

12.4. Set the strain rate to 6%/min (This is equivalent to 1.2mm/min) and start the test.

12.5. After the specimen fractures, degradation is observed, or maximum traveling distance is reached (whichever comes first), stop the test and remove the specimen from the loading frame.

12.6. The extensibility is identified as follows: When the specimen fractures (breaks into two pieces), the extensibility is easily identified as the strain at peak load (maximum stress). When the specimen does not fracture, but reaches a maximum stress and then flows without fracture, the extensibility is recorded as the strain corresponding to the maximum stress. When the specimen does not fracture or load reduction is not observed, the extensibility is recorded as the strain at the end of the traveling distance.

12.7. Repeat 12.3 to 12.6 for the remaining three specimens.

12.8. After testing is complete, discard the bituminous portions of the spent specimens and clean the end tabs by soaking them in solvent and wiping with a soft cloth. After wiping the end tabs, use a detergent soap solution to remove any oil film residue left by the cleaner material. Alternatively, use a degreasing spray cleaner. Clean the end tabs thoroughly. A grease film on the sealant bonding area can create a weak bond causing bond failures.

13. CALCULATIONS

13.1. For each test result, calculate the engineering stress-strain

$$\sigma_f = \frac{P_f}{A_0} \qquad (13.13)$$

$$\varepsilon_f = \frac{\Delta L_f}{L_0} \qquad (13.14)$$

where,

σ_f = peak stress;
P_f = measured load at peak;
A_0 = original cross-sectional area (=18mm^2);
ε_f = measured strain at peak load;
L_f = measured elongation at failure (ΔL); and

L_e = gauge length (=20.3mm).

13.2. For each test result, calculate the true stress-strain

$$\tilde{\varepsilon} = \frac{\Delta L_f}{L_0}. \quad (13.15)$$

$$\tilde{\sigma} = \frac{P_f}{A_i} = \frac{P \times e^{(\dot{\varepsilon} t)}}{A_0} \quad (13.16)$$

where,

$\tilde{\sigma}$ = true stress;
$\tilde{\varepsilon}$ = true strain;
P_f = measured load at peak;
A_0 = original cross-sectional area (=18mm^2);
$\dot{\varepsilon}$ = strain rate.

13.3. The extensibility is identified as $\tilde{\varepsilon}$.

13.4. Select the best three test results which give the best coefficient of variation of the extensibility. Calculate the mean and standard deviation for the selected three test results.

14. REPORT

14.1. Report the sealant name and supplier, lot number, date received, date sampled according to ASTM D5167.

14.2. Report the date and time of test, test temperature, rate of elongation, average extensibility and their standard deviation, peak load, and type of fracture (fracture or no fracture).

15. PRECISION AND BIAS

15.1. Confidence intervals of 95% should be constructed around the average of the calculated extensibility from the results of the four replicates. The closest three measurements will then be used to calculate the coefficient of variation while the fourth replicate will be discarded. A coefficient of variation less than 15% is desirable.

16. KEYWORDS

16.1. Hot-poured bituminous sealant; joint; crack; direct tension test; extensibility; strain energy density; low temperature; pavement maintenance.


Illinois Department
of Transportation


ILLINOIS
UNIVERSITY OF ILLINOIS AT URBANA-CHAMPAIGN